Targeting the extracellular HSP90 co-chaperone Morgana inhibits cancer cell migration and promotes anti-cancer immunity

Targeting the Extracellular HSP90 Co-Chaperone Morgana Inhibits Cancer Cell Migration and Promotes Anticancer Immunity

Laura Seclì [1], Lidia Avalle [1], Pietro Poggio [1], Giuseppe Fragale [1], Cristiana Cannata [1], Laura Conti [1], Andrea Iannucci [2 3], Giovanna Carrà [4], Cristina Rubinetto [1], Barbara Miniscalco [5], Emilio Hirsch [1], Valeria Poli [1], Alessandro Morotti [4], Marco De Andrea [2 6], Emilia Turco [1], Federica Cavallo [1], Federica Fusella [1], Mara Brancaccio [7]

[1] Department of Molecular Biotechnology and Health Sciences, University of Torino, Torino, Italy.
[2] CAAD-Center for Translational Research on Autoimmune and Allergic Disease, University of Eastern Piedmont, Novara, Italy.
[3] Department of Translational Medicine, University of Eastern Piedmont, Novara, Italy.
[4] Department of Clinical and Biological Sciences, University of Torino, Orbassano, Italy.
[5] Department of Veterinary Science, University of Torino, Torino, Italy.
[6] Department of Public Health and Pediatric Sciences, University of Torino, Torino, Italy.
[7] Department of Molecular Biotechnology and Health Sciences, University of Torino, Torino, Italy.
mara.brancaccio@unito.it

Abstract

HSP90 is secreted by cancer cells into the extracellular milieu, where it exerts protumoral activities by activating extracellular substrate proteins and triggering autocrine signals through cancer cell surface receptors. Emerging evidence indicates that HSP90 co-chaperones are also secreted and may direct HSP90 extracellular activities. In this study, we found that the HSP90 co-chaperone Morgana is released by cancer cells and, in association with HSP90, induces cancer cell migration through TLR2, TLR4, and LRP1. In syngeneic cancer mouse models, a mAb targeting Morgana extracellular activity reduced primary tumor growth via macrophage-dependent recruitment of CD8+ T lymphocytes, blocked cancer cell migration, and inhibited metastatic spreading. Overall, these data define Morgana as a new player in the HSP90 extracellular interactome and suggest that Morgana may regulate HSP90 activity to promote cancer cell migration and suppress antitumor immunity.

Significance:

This work suggests the potential therapeutic value of targeting the extracellular HSP90 co-chaperone Morgana to inhibit metastasis formation and enhance the CD8+ T-cell–mediated antitumor immune response.

Introduction

Cancer cells can survive in a stressful environment by adapting to hypoxia, starvation, and hostile physicochemical conditions that are able to induce proteotoxic stress. Indeed, cancer cells overexpress and are addicted to chaperone proteins (1, 2). HSP90 is an essential and ubiquitous chaperone with multiple intracellular roles, ranging from protein folding, buffering protein denaturation, and assisting signal transduction protein conformational changes (3). HSP90 binds as a dimer to substrate proteins, called HSP90 clients, promoting modifications in their structure in an ATP-dependent manner (3). A number of cofactors, called co-chaperones, regulates HSP90 conformational changes and enzymatic activity and helps recruiting specific client proteins (3). For its crucial function in sustaining cancer cell survival and expansion (2), HSP90 has long been regarded as an attractive target for cancer treatment, but no HSP90 inhibitor has so far been approved for therapeutic use, due to severe adverse effects (4). HSP90 can localize at the plasma membrane in cancer cells and may regulate membrane properties, formation of membrane microdomains, and intracellular signaling (5, 6). Notably, HSP90 can be secreted by a wide number of cancer cell lines and human tumors (7) and it has been recognized as an early and accurate pan cancer biomarker in the plasma of patients with cancer (8, 9). From the extracellular milieu, HSP90 exerts a protumoral activity with a dual mechanism. On one hand, it modifies the tumor microenvironment by chaperoning and activating-specific extracellular client proteins, such as metalloproteinases (MMP; 10–13), fibronectin (14), the pro-form of tissue plasminogen activator (15) and lysil oxidase-like protein 2 (16). On the other hand, extracellular HSP90 (eHSP90) binds to several cancer cell surface receptors, among them the Low-density lipoprotein receptor–related protein-1 (LRP1, also known as CD91) and toll-like receptors (TLR) 2 and 4 (1). This binding unleashes signal transduction pathways promoting cancer cell survival, epithelial-to-mesenchymal transition, cell migration, and invasion (17–22). Of note, therapeutic approaches targeting eHSP90 have proven effective in preclinical models (23–25), underscoring the importance of deepening the study of eHSP90 functions, refining, and expanding the repertoire of strategies to modulate its action.

Morgana is an HSP90 co-chaperone protein encoded by the *CHORDC1* gene, belonging to the family of CHORD (cysteine- and histidine-rich domains) containing proteins (26–28). Besides CHORD domains, Morgana possesses a C-terminal CS (CHORD and Sgt1 containing) domain (26), homologous to the small chaperones α-crystallin and p23 (29). Morgana displays a high degree of phylogenetic conservation, from plants to mammals, and is essential for mouse and Drosophila development (30). Inside the cell, Morgana binds to HSP90 (27, 28, 31, 32) and regulates different signal transduction pathways. Inhibiting Rho kinases (30, 33) and activating AKT (33) and NF-κB (34), Morgana prevents centrosome overduplication and promotes cell

survival. In cancer, Morgana plays both oncogenic and oncosuppressive roles, depending on the cellular context. Although Morgana haploinsufficiency in mice causes a myeloproliferative neoplasm similar to chronic myeloid leukemia (35), its overexpression in breast cancer correlates with tumor aggressiveness and poor prognosis (33, 34). In other tumor types, the impact of Morgana is still unclear; however, TCGA dataset analysis indicates that Morgana expression levels correlate with poor prognosis and worse clinical parameters in several human tumors, including kidney renal carcinoma, breast invasive carcinoma, lung cancer, and melanoma.

Here, we found that Morgana is secreted by cancer cells through an unconventional pathway and that extracellular Morgana (eMorgana) induces cancer cell migration in an HSP90-dependent manner, via TLR2, TLR4, and LRP1. To specifically block Morgana extracellular protumorigenic function, we generated and characterized an anti-Morgana mAb (mAb 5B11B3) that is able to interfere with cancer cell migration. In vivo, mAb 5B11B3 was able to inhibit primary tumor growth by promoting anticancer immunity, as well as to blunt the ability of cancer cells to form metastasis in preclinical cancer models.

Materials and Methods

Cell culture

Cell lines MCF10A, MCF7, BT549, MDA-MB-231, 4T1, and CT26 were purchased from the ATCC and E0771 were obtained from Tebu-Bio. All cells were maintained below passage number 20. Cells were routinely tested for *Mycoplasma* contamination.

Conditioned medium

A total of 2×10^6 cells were plated in a 100-mm dish and allowed to settle for 24 hours. Cells were then refed with 10 mL serum-free medium and 1% MEM Non-Essential Amino Acids Solution (Thermo Fisher Scientific, ×100) and incubated for 48 hours at 37°C. Conditioned medium (CM) was collected and concentrated at 2,000 × g by centrifugation with Vivaspin 20 centrifugal concentrator MWCO10,000 Da (Sigma-Aldrich) up to 1 mL. For immunoprecipitation, 1 mL of CM was incubated with 5 µg of antibody or control IgG. 10 µg mL^{-1} of Brefeldin A was added to the cell medium for 5 hours, and then CM and cell total extract were analyzed by Western blotting. Uncropped images of blots are shown in Supplementary Fig. S7.

Western blotting

For Western blot analysis, cells were lysed in TBS with 1% Triton X-100, plus phosphatase and protease inhibitors. Total protein extracts (30–50 µg) or concentrated CM (50 µL) were analyzed by Western blotting and detected by the chemiluminescent reagent LiteAblot (Euro-clone).

Coimmunoprecipitation experiments

Total protein extracts (500 µg) or CM (200 µg) were incubated overnight at 4°C with 5 µg of primary antibodies, then protein G-coated sepharose was added for 45 minutes (GE Healthcare). Beads were washed 10 times in lysis buffer for total extract or TBS 10% glycerol for immunoprecipitations from CM and resuspended in laemmli buffer.

Coimmunoprecipitation of HSP90 and rMorgana from cancer cell surface were performed as follows: MDA-MB-231 shMorg cells were treated with 0.1 µmol/L of mbp or rMorgana (2 hours, 4°C), crosslinked with DTSSP (1 mmol/L, 2 hours, 4°C) and lysed with CHAPS buffer (1% CHAPS, 120 mmol/L NaCl, 2 mmol/L EDTA). Lysates were subjected to immunoprecipitation as described above.

Pull down assay

For TLR2 pull down experiments, amylose resin (New England Biolabs) was incubated with 10 µg of mbp or mbp-Morgana (rMorgana) recombinant proteins for 1 hour at 4°C. Then 0.3 µg of TLR2 recombinant protein (R&D Systems, 2616-TR-050) was added and incubated 2 hours at 4°C. Beads with bound proteins were washed 10 times with TBS 1% Triton X-100, eluted in SDS sample buffer and resolved by SDS-PAGE on gradient gels.

For LRP1 pull down experiments, Protein A/G agarose beads (Santa Cruz Biotechnology) were incubated with 2.5 µg of LRP1 recombinant protein (R&D Systems, 5395-L4–050) for 1 hour at 4°C. Then 0.5 µg of mbp or mbp-Morgana recombinant proteins were diluted in MDA-MB-231 CM or in unconditioned DMEM, added to the beads and incubated for 2 hours at 4°C. Beads with bound proteins were washed ten times with TBS 1% Triton X-100, eluted in SDS sample buffer and resolved by SDS-PAGE on gradient gels.

Wound-healing assay

MDA-MB-231, BT549, CALU-1, E0771, 4T1, and CT26 cells were cultured in 6-well plates. When 90% confluent, cells were starved 24 hours. Then, a wound was scratched in the center of the cell monolayer by a sterile plastic pipette tip. Serum-free medium plus 1% MEM non-essential amino acids solution (Thermo Fisher Scientific, ×100) was placed in each well with either the vehicle control PBS, 0.1 µmol/L recombinant mbp protein or 0.1 µmol/L recombinant mbp-Morgana protein (rMorgana), in combination or not with the neutralizing antibody against TLR2 (30 ng mL^{-1}), TLR4 (100 ng mL^{-1}), TLR5 (100 ng mL^{-1}), HSP90 (100 ng mL^{-1}), HER2 (1 µg mL^{-1}), EGFR (1 µmol/L) or with 17AAG (1 µmol/L) following the manufacturer's instructions. Antibodies against Morgana and antibodies against mbp were used at 15 µg mL^{-1} (when not specified). The image of the wound was captured at time 0 and after 24 hours using live-cell imaging microscopy (Carl Zeiss). The percentage of wound closure was calculated using Axio Vision program or ImageJ with Wound-

Healing Size Tool. Representative images of wound-healing experiments are shown in Supplementary Fig. S6.

Immunofluorescence

GFP shMorg cells (30×10^3) were cultured in 24-well plates. After 24 hours, cells were treated with mbp or mbp-Morgana (0.1 µmol/L) in serum-free medium for 24 hours. Cells were fixed with PFA 4% and saturated with PBS 1% BSA. A primary antibody against mbp (1 h RT) was used to stain recombinant proteins on the cell membrane without permeabilization. Secondary antibody was added and DAPI staining was performed. Glasses were analyzed with Z-stack using a confocal microscope (Leica SP8).

Antibody characterization

To characterize the mAb 5B11B3, Pierce Rapid Isotyping kit mouse (Thermo Fisher) and IsoQuick Kits for Mouse Monoclonal Isotyping (Sigma) were used, following the manufacturer's instructions. mAb sequencing was performed by GenScript Biotech (the Netherlands). The mRNA was isolated from hybridoma cells with TRIzol Reagent and retrotranscribed to cDNA using anti-sense primers or universal primers for isotypes following the technical manual of FirstScript 1st Strand kit. Regions codifying antibody fragments VH, VL, CH e CL were amplified and cloned in a standard sequencing vector. For each fragment, a minimum of five independent clones were sequenced and then these sequences were aligned to get the final sequence report with CDR region annotated.

ELISA assay

Recombinant human or mouse mbp-Morgana (15 µg mL^{-1} in 100 µL) were used to coat a 96-well plate at 4°C overnight. After washing 3 times with PBS, saturation was performed with PBS 3% BSA for 1 hour at room temperature. After washing 3 times with PBS, serial dilutions of the primary antibody (5B11B3 or control IgG in PBS 1% BSA) from 10 µg mL^{-1} to 0, were added to the plate for 1 hour at room temperature. After washing 3 times with PBS, secondary antibody horseradish peroxidase anti-Mouse IgG in PBS (Sigma, A4416, 1:4,000) was used for 1 hour at room temperature and reveled with 3,3′,5,5′-Tetramethylbenzidine (TMB, Sigma, T0440). The reaction was blocked with HCl (40%) and absorbance measured at 450 nm.

Blood analysis

C57BL/6 and BALB/c mice were injected intravenously with 100 µg of the mAb 5B11B3 or control IgG, 3 times per week. After 1 month, animals were sacrificed, and blood collected for the analysis.

In vivo tumor and metastasis assays

Mouse model to study circulating tumor cells

MDA-MB-231 human breast cancer cells injected subcutaneously in immunodeficient NOD-SCID IL2Rgnull (NSG) mice (Fig. 2J).

A total of 1 × 10^6 MDA-MB-231 cells infected with a lentivirus carrying GFP were inoculated subcutaneously in 7-week-old female immunodeficient NSG mice. After tumor growth (25 mm^3), animals were treated with vehicle (PBS), recombinant mbp (100 µg), recombinant mbp-Chord (N-terminal Morgana domain; 100 µg) or recombinant mbp-Morgana protein (100 µg) in PBS. Animals were treated four times and after 24 hours from the last injection, mice were sacrificed, and the blood was collected in heparin. After lysis of red blood cells, blood samples were analyzed by flow cytometry for GFP-positive cells. Flow cytometry analyzes were carried out on a BD Celesta (Becton Dickinson).

Mouse model for experimental metastasis assay

MDA-MB-231 human breast cancer cells injected subcutaneously in immunodeficient NSG mice (Fig. 3D).

Experimental metastasis assay was performed by injecting 5 × 10^5 MDA-MB-231 cells (empty or downregulated for Morgana) into the tail vein of 7-week-old female immunodeficient NSG mice. After 4 days, animals were treated with mAb 5B11B3 or control IgG (100 µg, intravenous injection, 4 treatments each other day) or PBS. After 19 days mice were sacrificed and lungs collected were formalin-fixed and paraffin-embedded (FFPE), sectioned, and stained with hematoxylin and eosin (H&E). Metastases were evaluated with an Olympus BH2 microscope, on the entire lungs section. Metastatic burden was evaluated as the percentage of lung metastatic area using ImageJ Software (Universal Imaging Corporation).

Mouse model for spontaneous metastasis assays

4T1 mouse breast cancer cells injected in BALB/c mice (Supplementary Fig. S3N).

A total of 2 × 10^5 4T1 cells infected with a lentivirus carrying GFP were inoculated subcutaneously in syngeneic BALB/c mice. After tumor growth (120 mm^3), animals were treated with intratumor injections of recombinant mbp (100 µg), or recombinant mbp-Morgana (100 µg) in PBS. Animals were treated four times (2 times a week), and after 24 hours from the last injection, mice were sacrificed and lungs collected. Metastases were evaluated with an Olympus BH2 microscope, on the entire lungs section. Metastatic burden was evaluated as the percentage of lung metastatic area using ImageJ Software (Universal Imaging Corporation).

Mouse models for preventive treatment

E0771 mouse breast cancer cells injected subcutaneously in C57BL/6 mice and 4T1 breast cancer cells injected subcutaneously in BALB/c mice for spontaneous metastasis assays (Fig. 3H; Supplementary Fig. S3P).

A total of 2 × 10^5 E0771 (empty or downregulated for Morgana) and 1 × 10^5 4T1 cells were inoculated subcutaneously in syngeneic C57BL/6 and BALB/c mice. After 1 day, mice were treated with mAb 5B11B3 or control IgG (100 μg, intravenous injection, 3 times per week). Animals were sacrificed after 20 and 15 days, respectively, and tumors collected for weight measurement.

Mouse models for therapeutic treatment

E0771 mouse breast cancer cells injected subcutaneously in C57BL/6 mice and CT26 mouse colon cancer cells injected subcutaneously in BALB/c mice (Fig. 3I–L).

For the therapeutic experiment, E0771 (2 × 10^5) and CT26 (2 × 10^5) were subcutaneously injected in syngeneic C57BL/6 and BALB/c mice, respectively, and after primary tumor development (size around 15 mm^3), animals were treated with mAb 5B11B3 or control IgG (100 μg, intravenous injection, 3 times per week) measuring tumor volume during the entire experiment. Animals were sacrificed (at 40 and 25 days, respectively) and tumors collected for weight measurement. For the assessment of metastasis, organs were FFPE, sectioned, and stained with H&E. Metastases were evaluated with an Olympus BH2 microscope.

Mouse model to study the efficacy of mAb 5B11B3 in inhibiting metastasis formation

MDA-MB-231 human breast cancer cells injected subcutaneously in NSG mice (Fig. 4C and D).

A total of 1 × 10^6 MDA-MB-231 cells were inoculated subcutaneously in 7-week-old female immunodeficient NSG mice and, after 20 days, animals were treated with mAb 5B11B3 or control IgG (100 μg by intravenous injection, 2 times per week). After 24 days, mice were sacrificed, and tumors weighted.

Mouse models to study immune cell recruitment in the tumor

E0771 mouse breast cancer cells injected subcutaneously in C57BL/6 mice and CT26 mouse colon cancer cells injected subcutaneously in BALB/c mice (Fig. 4E and F; Supplementary Fig. S4F–S4L; Fig. 5A–D; Supplementary Fig. S5A–S5F and S5J–S5K).

E0771 (2 × 10^5) and CT26 (2 × 10^5) were subcutaneously injected in syngeneic C57BL/6 and BALB/c mice, respectively, and after primary tumor development (size around 15 mm^3), animals were treated with mAb 5B11B3 or control IgG or in some experiments with 5B11B3 Fab or IgG Fab (100 μg, intravenous injection) 1 or 3 times and then were sacrificed. Tumors were weighted and the immune composition was analyzed by flow cytometry.

Mouse models to study the role of macrophages

E0771 mouse breast cancer cells injected subcutaneously in C57BL/6 and CT26 mouse colon cancer cells injected subcutaneously in BALB/c mice (Fig. 5E–I; Supplementary S5G–S5I).

For macrophage depletion in vivo, E0771 (2×10^5) and CT26 (2×10^5) were subcutaneously injected in syngeneic C57BL/6 mice and BALB/c mice, respectively. After primary tumor development (size around 15 mm^3), animals were treated with clodronate liposomes in PBS (Liposoma, CP-010–010) 100 µg per 10 gr/mouse. After 4 days, mice were treated with mAb 5B11B3 or control IgG (100 µg, tail vein injection) 3 times and then were sacrificed. Tumors were weighted and the immune composition was analyzed by flow cytometry. Otherwise, after primary tumor development (size around 15 mm^3), animals were treated with clodronate liposomes in PBS (Liposoma, CP-010–010) 100 µg per 10 gr/mouse. After 3 days, mice were treated with mAb 5B11B3 or control IgG (100 µg, tail vein injection, 3 times per week) measuring tumor volume during the entire experiment. Animals were sacrificed at 18 days and tumors collected for weight measurement. For the assessment of metastasis, organs were FFPE, sectioned, and stained with H&E. Metastatic burden was evaluated.

A detailed sketch of each experiment is provided in each figure.

Murine bone marrow macrophages

Bone marrow from wild-type C57BL/6 mice was harvested from freshly isolated femurs, tibiae, and humeri. After removal of connective tissues and muscles, bone marrow was flushed, and single-cell suspensions were made by passing bone marrow through a sterile 70 µmol/L filter (BD Falcon). Macrophages were differentiated by incubating bone marrow cells for 7 days with complete RPMI, supplemented with 15% L929-CM (containing M-CSF). Macrophages were harvested after incubation with PBS 5 mmol/L EDTA. Macrophages were seeded in 6-mm dishes for live-cell imaging or on glasses in 24-well plates for analysis under fluorescence microscope.

Coculturing experiments

ADPh assay

Macrophages and E0771 cancer cells were, respectively, labeled with 5 µmol/L CellTracker Orange Dye or CellTracker Green CMFDA Dye (Thermo Fisher) following the manufacturer's protocol. Cells were cocultured in an effector to target ratio (E:T) of 4:1 with mAb 5B11B3 or control IgG (10 µg). Cells were fixed at different time points, cell nuclei marked with DAPI and analyzed using fluorescence microscope Apotome (Zeiss). For live-cell imaging, macrophages and cancer cells (E0771 or CT26) were cocultured in an E:T ratio of 4:1 with mAb 5B11B3 or control IgG (10 µg) and followed in bright field for 24 hours.

ADCC assay

NK cells were preactivated by gavage of 200-µg Tilorone (Sigma-Aldrich) in WT C57BL/6 mice 24 hours before the harvest of splenocytes. Mice were sacrificed and splenocytes were isolated. E0771 were labeled with 2 µmol/L CellTrace CFSE (Thermo Fisher) and plated 5×10^3 cells per well in 96-well plates. Splenocytes were plated in the same wells using 3 different E:T ratios (50:1,

100:1, and 200:1) in presence of the mAb 5B11B3 or control IgG (10 µg). After 16 hours, lived E0771 cells from each well were collected and analyzed by flow cytometry.

Fab preparation

Pierce Fab Preparation Kit (Thermo Fisher) was used to purify Fab fragments of mAb 5B11B3 and control IgG. E0771 (2×10^5) and CT26 (2×10^5) were, respectively, subcutaneously injected in syngeneic C57BL/6 mice and BALB/c mice, and after primary tumor development (size around 15 mm^3), animals were treated with mAb 5B11B3, control IgG, Fab 5B11B3 or Fab control IgG (100 µg, tail vein injection) 1 time and then were sacrificed. Tumors were weighted and the immune composition was analyzed by flow cytometry in both E0771 and CT26 models.

Statistical analysis

The data are presented as means ± SEM. For statistical analyzes, significance was tested using the Student *t* test, one-way ANOVA, and two-way ANOVA with Fisher LSD or Bonferroni *post hoc* test. A minimum value of $P < 0.05$ was considered statistically significant. Statistical analyzes were performed using GraphPad Prism 8.

Animal welfare

Mice were kept in pathogen-free conditions in the animal facility of the Molecular Biotechnology Center (University of Turin) under a 12-hour light/dark cycle, 55% ± 5% humidity, temperature 23°C ± 2°C, and provided with food and water ad libitum. Experiments with mice were carried out in accordance with the ethical guidelines of the European Communities Council Directive (2010/63/EU). Experimental approval was obtained from the Italian Health Ministry (540/2018-PR).

Results

Cancer cells secrete Morgana through unconventional pathways

The Cancer Cell Secretome database (36), collecting data from up to 35 high-throughput studies on 17 cancer types, highlights that the HSP90 co-chaperone Morgana can be detected in the CM of a number of cancer cell lines, including breast, lung, and colon cancer cells (Supplementary Fig. S1A). We confirmed the presence of Morgana in the medium of several human breast cancer cells (MDA-MB-231, BT549, HCC1937, MDA-MB-468), whereas a much lower amount was detected in the CM of noncancerous breast cells (MCF10; Fig. 1A). Similar results were obtained analyzing the CM of several lung cancer cells (Supplementary Fig. S1B).

We chose the widely used MDA-MB-231 and BT549 breast cancer cell lines to better characterize Morgana secretion. Other cytoplasmic proteins were absent from the extracellular media, ruling out the possibility of cytoplasmic content release due to cell damage. Besides HSP90, other Morgana

cytoplasmic interactors, such as IKKα, IKKβ, IκBα, and ROCK I, were undetectable in the CM (Fig. 1B). As demonstrated by immunoprecipitation experiments performed on MDA-MB-231 (Fig. 1C) and BT549 (Supplementary Fig. S1C) CM, Morgana interacts with HSP90 also in the extracellular milieu. Morgana is not secreted as a passive HSP90 passenger, because the downregulation of HSP90α, the main secreted isoform, did not affect Morgana release (Fig. 1D). HSP90 is mainly exported on the surface of exosomes (37) and, recently, Morgana has been found to be required for extracellular vesicle secretion (38). However, Morgana is not essential for HSP90 release, as demonstrated by its presence in the CM of MDA-MB-231 cells downregulated for Morgana (Fig. 1B; Supplementary Fig. S1D). Like other secreted chaperone proteins, Morgana lacks a signal peptide required for translocation into the endoplasmic reticulum. Accordingly, Brefeldin A, an inhibitor of the canonical ER–Golgi pathway, did not inhibit the secretion of Morgana and other chaperones, but it impaired the release of proteins endowed with a signal peptide, like MMP9, fibronectin, and laminin (Fig. 1E; Supplementary Fig. S1E). Of note, eMorgana and eHSP90 could be immunoprecipitated from CM without using detergents, indicating that at least a pool of these proteins is not incorporated into vesicles (Fig. 1C; Supplementary Fig. S1C).

Extracellular Morgana induces cancer cell migration through TLR2 and 4 and LRP1

Extracellular chaperones may act promoting cancer cell migration (6). In agreement, shRNA-mediated downregulation of Morgana reduces MDA-MB-231 and BT549 breast cancer cell migration (Fig. 2A; Supplementary Fig. S2A), without affecting proliferation (34). Cell migration was completely rescued by the addition in the medium of a recombinant Morgana fused to the maltose binding protein (rMorgana), whereas the maltose-binding protein (mbp) alone showed no effect (Fig. 2A; Supplementary Fig. S2A). Neither the Morgana N-terminal moiety, containing the two CHORD domains (rChord), nor the C-terminal one, consisting of the CS domain (rCS), were able alone to recover cell migration in Morgana downregulated cells, indicating that the full-length protein is required (Supplementary Fig. S2B). It is worth noting that all recombinant proteins were produced endotoxin free (39), to avoid confounding results due to the presence of lipopolysaccharide from bacterial extracts.

rMorgana-mediated rescue of cell migration was completely abolished by the addition of an eHSP90 blocking antibody (Fig. 2B; Supplementary Fig. S2C; ref. 40), suggesting that eMorgana acts mainly in association with eHSP90. The exogenously added rMorgana can be detected at the plasma membrane of breast cancer cells, forming multiple spots (Fig. 2C), suggesting a specific binding to cell surface receptors. This membrane-associated rMorgana can be co-immunoprecipitated with HSP90 after exposing cells to chemical cell impermeable cross-linkers, indicating that rMorgana and eHSP90 are associated when bound to the cell surface (Supplementary Fig. S2D). LRP1, TLR2 and 4, EGFR, and HER2 have been extensively described as eHSP90 receptors involved in cancer cell migration (1). After evaluating their expression in

MDA-MB-231 and BT549 breast cancer cells (Fig. 2D), we tested a possible involvement of these receptors in eMorgana-induced cancer cell motility. Blocking antibodies against TLR2 and 4, but not against TLR5, EGFR, and HER2 (Fig. 2E; Supplementary Fig. S2E–S2G), completely inhibited the ability of the rMorgana to induce migration in Morgana-silenced MDA-MB-231 and BT549 cells. shRNA-mediated depletion of LRP1 (Supplementary Fig. S2H) was also able to fully inhibit the activity of the rMorgana (Fig. 2F). These results suggest that the engagement of multiple receptors at the same time or a functional cross-talk among them is needed to activate eMorgana-dependent signals. Interestingly, the ability of LRP1 to function as a cross-talk receptor for activated TLRs has been recently described (41). In support of our previous data, we performed pull-down assays demonstrating a direct interaction between Morgana and the extracellular portion of TLR2 (Fig. 2G). Surface plasmon resonance analysis further demonstrated the direct association between TLR2 and Morgana, defining binding kinetics (KD = 1,243 10^{-5} mol/L; Fig. 2H; Supplementary Fig. S2I). However, we were not able to highlight a clear and specific interaction between Morgana and TLR4 extracellular domain. We also performed pull down experiments using a recombinant protein containing LRP1 complement-like repeat cluster II domain, known to be the target for most of LRP1 ligands. The results showed that Morgana binds to LRP1 cluster II domain only in presence of cancer cell CM (Fig. 2I; Supplementary Fig. S2J), suggesting that the interaction is mediated by additional components.

To evaluate the relevance of eMorgana in inducing cancer cell migration *in vivo*, NSG mice carrying established MDA-MB-231–derived tumors were subjected to intratumor injections of rMorgana, rChord (N-terminal Morgana) or mbp as control. After 4 treatments, mice injected with rMorgana showed twice as many circulating tumor cells in their bloodstream than mice injected with rChord or mbp (Fig. 2J). This result indicates that, also *in vivo*, the full-length eMorgana is required to promote cancer cell migration.

The treatment with an eMorgana-blocking antibody inhibits tumor growth and impairs metastasis formation

In the attempt to interfere with eMorgana protumorigenic functions, we generated a mAb against eMorgana (mAb 5B11B3). mAb 5B11B3 specifically recognizes both mouse and human Morgana (sharing 96% identity in their amino acidic sequence) in ELISA (Supplementary Fig. S3A), Western blot (Supplementary Fig. S3B) and immunoprecipitation assays (Supplementary Fig. S3C). mAb 5B11B3 is able to inhibit cancer cell migration *in vitro* in a dose-dependent manner, as tested in MDA-MB-231 (Fig. 3A) and BT549 (Supplementary Fig. S3D) breast cancer cell lines, as well as in the non–small cell lung cancer cell line CALU-1 (Supplementary Fig. S3E). Of note, the ability of mAb 5B11B3 to inhibit cancer cell migration was not further potentiated by the concomitant treatment with an eHSP90 blocking antibody or the cell permeable HSP90 inhibitor Tanespimycin (17AAG; Fig. 3B). We characterized mAb 5B11B3 as an IgG1 isotype with κ chain (Supplementary

Fig. S3F). The mAb recognizes amino acids 85–110 (25 amino acids out of 26 are conserved between human and mouse, Supplementary Fig. S3G) located in between the two Morgana Chord domains (Fig. 3C). The mAb 5B11B3 does not disrupt the association between Morgana and HSP90, as demonstrated by coimmunoprecipitation experiments (Supplementary Fig. S3H). mAb 5B11B3 did not alter cancer cell viability and proliferation *in vitro* (Supplementary Fig. S3I and S3J). Injection of mAb 5B11B3 for 30 days did not affect liver, pancreas and kidney functions in C57BL/6 (Supplementary Fig. S3K) nor in BALB/c mice (Supplementary Fig. S3L), supporting the feasibility of in vivo treatments.

As a first attempt to test the ability of mAb 5B11B3 to inhibit tumor cell migration, we took advantage of an experimental metastasis model in immunocompromised mice. The formation of metastasis in this assay mainly depends on the ability of cancer cells to survive in the blood stream, to migrate across the endothelial barrier and to proliferate in the secondary organ. NSG mice were injected intravenously with MDA-MB-231 or MDA-MB-231 downregulated for Morgana and treated twice a week (starting 4 days after cell inoculation) with mAb 5B11B3 or with a control antibody. mAb 5B11B3 treatment significantly lowered the lung metastatic burden in mice carrying MDA-MB-231-derived tumors, but not in mice inoculated with MDA-MB-231 cells downregulated for Morgana (Fig. 3D). Notably, downregulation of Morgana resulted in lower metastatic burden than in parental MDA-MB-231 cells, likely due to the role of intracellular Morgana in sustaining the NF-κB pathway, as previously demonstrated (34).

Encouraged by this result, we moved to immunocompetent mouse models to further investigate the impact of Morgana on tumor progression. Analyzing the CM of different murine cancer cells, we found that Morgana is secreted at higher levels by E0771 (breast), LLC (lung), B16 (melanoma) and CT26 (colon) compared with 4T1 (breast) cells (Fig. 3E). We demonstrated that mAb 5B11B3 affects cell migration *in vitro* in E0771 (Fig. 3F) and CT26 (Supplementary Fig. S3M), but not in 4T1 cells (Fig. 3G). Moreover, injection of rMorgana in 4T1-derived tumors increases the lung metastatic burden in BALB/c mice (Supplementary Fig. S3N).

E0771 cells were injected subcutaneously in C57BL/6 mice, followed by treatment with mAb 5B11B3 or control IgG, starting from day 1 after the inoculum. After 20 days, we observed a robust reduction of primary tumor growth in mAb-treated animals (Fig. 3H). This effect depends on Morgana, because mAb 5B11B3 treatment failed to interfere with the growth of tumors derived from E0771 silenced for Morgana (Fig. 3H). Note that Morgana downregulation in mouse cancer cell lines does not impair cell proliferation *in vitro* (Supplementary Fig. S3O; ref. 34). To further investigate the presence of potential mAb 5B11B3 off-target activities leading to tumor growth impairment, we used the mouse model generated by subcutaneous injection of breast cancer 4T1 cells, which express high Morgana levels but secrete much less eMorgana with respect to E0771 cells (Fig. 3E). In this model, the treatment with mAb 5B11B3 does not reduce tumor volume

compared with control IgG treatment (Supplementary Fig. S3P), supporting the notion that eMorgana is the therapeutic target of mAb 5B11B3.

To evaluate the therapeutic potential of mAb 5B11B3 treatment, we set up curative protocols in which treatments with mAb 5B11B3 or control IgG started when E0771-derived tumors became palpable and lasted for 4 weeks. The treatment with mAb 5B11B3 caused a significant inhibition of the primary tumor growth (Fig. 3I and J) and a decrease in lung metastasis (Fig. 3K).

Similar results were obtained with CT26 colon cancer cells, which also secrete Morgana in the CM (Fig. 3E), suggesting that the same mechanism applies to distinct cancer types (Fig. 3L).

The mAb 5B11B3 induces macrophage and CD8+ T lymphocyte recruitment in the primary tumor

It is well known that antibodies, in addition to direct therapeutic activities, may promote immune-mediated cancer cell killing (42). Because the treatment with mAb 5B11B3 does not affect cancer cell apoptosis and proliferation *in vitro* (Fig. 4A and B; Supplementary Fig. S4A–S4D) and does not reduce MDA-MB-231 tumor volume and weight in immunodeficient mice (Fig. 4C and D), we hypothesized that the immune system plays an active role in mAb 5B11B3 therapeutic activity. The fragment crystallizable region of antibodies (Fc region, FcR) may induce immune effector cell recruitment in the tumor and promote their anticancer activities, by binding specific receptors (FcRs; ref. 43). Some therapeutic antibodies trigger antibody-dependent cell-mediated cytotoxicity (ADCC), a mechanism by which FcR-bearing NK, macrophages and other effector cells recognize antibody-coated cells and kill them (42). ADCC *in vitro* assays showed that mAb 5B11B3 did not trigger significant cytotoxic activities in murine NK cells activated *in vivo* (Supplementary Fig. S4E). Consistently, after 24 hours from a single injection in mice of mAb 5B11B3 (100 μg), no differences were observed in the presence of NK cells in E0771 and CT26-derived subcutaneous tumors (Supplementary Fig. S4F–S4J). In these experimental conditions, macrophages were the only immune cells recruited into the tumor (Fig. 4E and F; Supplementary Fig. S4K and S4L), suggesting their involvement in mAb 5B11B3 anticancer activity. Macrophages express FcRs that can mediate the direct killing of cancer cells by antibody-dependent phagocytosis (ADPh; ref. 44). The injection of mAb 5B11B3 lacking the FcR (mAb 5B11B3 Fab fragments) in mice carrying palpable E0771 (Fig. 4E and F) and CT26-derived tumors (Supplementary Fig. S4K and S4L), was not effective in recruiting macrophages, indicating that macrophage recruitment is mediated by the Fc portion of the antibody. To investigate whether mAb 5B11B3 exerts its therapeutic activity through a macrophage-mediated mechanism, we performed co-culture experiments with E0771 tumor cells and bone marrow–derived macrophages (BMDM). The presence of mAb 5B11B3, but not that of the control IgG, increased the ability of macrophages to interact with cancer cells (Fig. 4G). Consistently, after 24 hours of co-culture, the number of E0771 cells was 4 times lower when mAb 5B11B3 was added to the culture (Fig. 4H).

Beside their ability to phagocyte cancer cells, activated macrophages may secrete cytokines able to engage and activate other immune cells with antitumor activity (45). To maximize responses, treatment with mAb 5B11B3 or control IgG was repeated 3 times in C57BL/6 mice injected subcutaneously with E0771 cells. In this condition, we found a significant increase in the percentage of $CD8^+$ T lymphocytes compared with controls (Fig. 5A and B; Supplementary Fig. S5A). Next, we shifted to an orthotropic mouse model, by injecting E0771 in the mammary fat pad of C57BL/6 mice. In line with our previous results, $CD8^+$ T lymphocytes doubled in the tumor when mice were treated with mAb 5B11B3, whereas the number of FOXP3+ T regulatory lymphocytes remained unchanged (Fig. 5C and D). Similar results were obtained by treating mice carrying CT26-derived tumors with mAb 5B11B3 (Supplementary Fig. S5B–S5D). Of note, downregulation of the Morgana antigen in tumors totally abolished the mAb 5B11B3-induced recruitment of $CD8^+$ T lymphocytes (Supplementary Fig. S5E and S5F).

Depletion of macrophages by clodronate liposome injection, abrogated CD8+ T lymphocyte recruitment in mAb 5B11B3-treated mice (Fig. 5E and F; Supplementary Fig. S5G–S5I), implying that their engagement depends on macrophages. To evaluate whether mAb 5B11B3-dependent immune cell recruitment impairs tumor growth, we monitored tumor volume in mice treated with mAb 5B11B3 and clodronate liposome injections (Fig. 5G). Macrophage depletion significantly affected the ability of mAb 5B11B3 to inhibit tumor growth (Fig. 5G and H, pink squares vs. green squares) and metastasis formation (Fig. 5I).

In conclusion, we demonstrated that the co-chaperone Morgana is unconventionally secreted by several cancer cells and that, in complex with HSP90, promotes cancer cell migration via TLR2, TLR4, and LRP1. We generated a mAb that is able to block eMorgana extracellular function and to inhibit tumor growth by inducing ADPh and macrophage-dependent recruitment of $CD8^+$ T lymphocytes in the tumor.

Discussion

When released by cancer cells, HSP90 may exert both oncosuppressive and oncogenic functions. On the one hand, HSP90 plays a role in presenting oncogenic antigens to antigen-presenting cells, increasing their ability to activate immune responses, promoting antitumor immunity (46). On the other hand, it promotes cancer cell survival, migration and invasion, by activating specific extracellular clients and by signaling through cancer cell receptors (1, 6). The molecular mechanisms by which eHSP90 plays these different functions and binds to different interactors are still unclear. Emerging evidence indicate that, also in the extracellular milieu, co-chaperones play a

crucial function in directing HSP90 activities. Indeed, some intracellular HSP90 co-chaperones, such as Aha1 (11), p23, Hop (12, 47), Cdc37 (48), and clusterin (21) are secreted by cancer cells and assist eHSP90. Aha1, p23, and Hop are involved in MMP2 activation (11, 12), Cdc37 in the regulation of the kinase receptors HER2 and EGFR (48) and clusterin in LRP1 stimulation (21). These indications suggest that cancer cells export a repertoire of co-chaperones that bind to eHSP90 and direct its association with extracellular clients and surface receptors, ultimately dictating its activity (1). Our results suggest that Morgana directs eHSP90 activity on TLR2, 4 and LRP1, promoting cancer cell migration. The fact that TLR2, TLR4, and LRP1 are all essential to unleash Morgana/HSP90-dependent signals is suggestive of a coordinated cross-talk among these receptors. Interestingly, the ability of LRP1 to function as a cross-talk receptor for activated TLRs and its requirement in triggering uncanonical signaling, have been recently highlighted (41). We found that Morgana binds directly to TLR2, whereas its interaction with LRP1 is likely mediated by a component of the cancer cell CM. The fact that HSP90 binds to both Morgana and LRP1 makes it a reasonable candidate for this role, however, further studies are required to prove this hypothesis.

Although we confirmed the interaction between Morgana and TLR2 or LRP1, we were not able to measure a direct interaction with TLR4. This may depend on the fact that TLR4 require coreceptors to mediate the binding with its ligand (49) or that TLR4 is indirectly activated by TLR2 and LRP1. Further studies are needed to define the signal transduction pathways involved in transducing Morgana/HSP90 signals, also in view of the fact that we could not detect the activation of canonical TLR signaling.

Therapeutic approaches targeting eHSP90 have been used successfully in preclinical models (1, 10, 23, 25). The use of a mAb against eHSP90α almost totally blocks the growth of breast cancer cells in mice when treatment is started concomitantly to cancer cell inoculation and significantly inhibits cancer expansion in a therapeutic setting (23). The idea to target extracellular HSP90 co-chaperones *in vivo* is arising as a promising anticancer treatment, virtually able to block specific HSP90 extracellular functions (21). In the attempt to inhibit Morgana extracellular activity, we generated and selected a mAb against Morgana, able to impair cancer cell migration. In syngeneic mouse models, the antibody against Morgana significantly inhibited tumor growth, by breaking the immunosuppressive environment imposed by the tumor. Because we started treatments when tumors were still small (15 mm^3), further studies are required to assess the efficacy of the treatment in more advanced stages of cancer growth. Nevertheless, our data indicate that mAb 5B11B3 attracts and activates macrophages in the tumor microenvironment through its Fc portion. Activated macrophages exert a double anticancer activity by phagocyting cancer cells and secreting chemokines, which promote a second wave of leukocyte recruitment. Indeed, in response to mAb 5B11B3 treatment, we detected a macrophage-dependent increase in CD8+ T

lymphocytes in the tumor. Of note, there is not a clear identity in macrophage subpopulations recruited in response to mAb 5B11B3 treatment. In the CT26 mouse model, we highlighted a significant increase in the MHC II and CD206 double-positive macrophage population, whereas in the E0771 model different macrophage subtypes were involved. This is in line with recent findings, pointing to a complex spectrum of macrophage polarization in tumors, in which M1 and M2 signatures seem to correlate instead of being alternative (50). Myeloid-derived suppressor cells (MDSC) are immature myeloid cells able to inhibit innate and adaptive immunity and favor tumor growth. We noticed that mAb 5B11B3 treatment in the breast cancer mouse model, but not in the colon cancer model, significantly decreased MDSCs in the primary tumor. This suggests that in addition to $CD8^+$ T lymphocytes recruitment, in some contexts, mAb 5B11B3 may promote their function by inhibiting immunosuppressive signals.

Overall, our data define Morgana as a new intriguing player in the HSP90 extracellular interactome and suggest that Morgana may drive HSP90 to promote cancer cell migration through TLRs and LRP1. These findings open a number of exciting questions related to the molecular mechanisms by which extracellular co-chaperones may force specific HSP90 structural conformations and how HSP90 may promote the activation of surface receptors. In this regard, our data suggest that HSP90 triggers a multireceptor cross-talk, resulting in an unconventional signaling. Finally, we demonstrated that targeting extracellular co-chaperones through therapeutic antibodies represents a successful approach able to block the extracellular chaperone protumorigenic activity and to activate the immune system against the tumor.

Authors' Disclosures

L. Seclì reports a patent 102020000021667 pending. E. Hirsch reports personal fees from Kither Biotech outside the submitted work. E. Turco reports a patent for 102020000021667 pending. F. Fusella reports a patent 102020000021667 pending. M. Brancaccio reports grants from Regione Piemonte and AIRC Italian Association for Cancer Research during the conduct of the study, as well as has a patent 102020000021667 pending. No disclosures were reported by the other authors.

Acknowledgments

The authors would like to thank Valeria Caneparo at CAAD—Center for Translational Research on Autoimmune and Allergic Disease (Novara, Italy) for assistance with SPR analyses. They thank Marta Gai for help with confocal microscopy. The authors are also grateful to Flavio Cristofani and Antonellisa Sgarra for assistance with animal experiments. This work was supported by Digital

Technology for Lung Cancer Treatment (DEFLeCT; to M. Brancaccio, V. Poli, and F. Cavallo), by AIRC (IG 24930 to M. Brancaccio, IG 21468 to F. Cavallo, and IG 24851 to V. Poli), L. Seclì was supported by a fellowship from AIRC (Federica Cipollat Mis ID: 24216), G. Carrà was supported by a fellowship from AIRC (Giorgio Felisari ID: 25254).

References

1. Calderwood SK. Heat shock proteins and cancer: intracellular chaperones or extracellular signalling ligands?Philos Trans R Soc Lond B Biol Sci 2018;373:20160524.
2. Whitesell L, Lindquist SL. HSP90 and the chaperoning of cancer. Nat Rev Cancer 2005;5:761–72.
3. Schopf FH, Biebl MM, Buchner J. The HSP90 chaperone machinery. Nat Rev Mol Cell Biol 2017;18:345–60.
4. Bickel D, Gohlke H. C-terminal modulators of heat shock protein of 90kDa (HSP90): state of development and modes of action. Bioorg Med Chem 2019;27:115080.
5. Horvath I, Multhoff G, Sonnleitner A, Vigh L. Membrane-associated stress proteins: more than simply chaperones. Biochim Biophys Acta 2008;1778:1653–64.
6. Secli L, Fusella F, Avalle L, Brancaccio M. The dark-side of the outside: how extracellular heat shock proteins promote cancer. Cell Mol Life Sci 2021;78:4069–83.
7. Wang X, Song X, Zhuo W, Fu Y, Shi H, Liang Y, et al The regulatory mechanism of Hsp90alpha secretion and its function in tumor malignancy. Proc Natl Acad Sci U S A 2009;106:21288–93.
8. Liu W, Li J, Zhang P, Hou Q, Feng S, Liu L, et al A novel pan-cancer biomarker plasma heat shock protein 90alpha and its diagnosis determinants in clinic. Cancer Sci 2019;110:2941–59.
9. Li W, Tsen F, Sahu D, Bhatia A, Chen M, Multhoff G, et al Extracellular Hsp90 (eHsp90) as the actual target in clinical trials: intentionally or unintentionally. Int Rev Cell Mol Biol 2013;303:203–35.
10. Stellas D, El Hamidieh A, Patsavoudi E. Monoclonal antibody 4C5 prevents activation of MMP2 and MMP9 by disrupting their interaction with extracellular HSP90 and inhibits formation of metastatic breast cancer cell deposits. BMC Cell Biol 2010;11:51.
11. Baker-Williams AJ, Hashmi F, Budzynski MA, Woodford MR, Gleicher S, Himanen SV, et al Co-chaperones TIMP2 and AHA1 competitively regulate extracellular HSP90:client MMP2 activity and matrix proteolysis. Cell Rep 2019;28:1894–906.
12. Sims JD, McCready J, Jay DG. Extracellular heat shock protein (Hsp)70 and Hsp90alpha assist in matrix metalloproteinase-2 activation and breast cancer cell migration and invasion. PLoS ONE 2011;6:e18848.

13. Song X, Wang X, Zhuo W, Shi H, Feng D, Sun Y, et al The regulatory mechanism of extracellular Hsp90{alpha} on matrix metalloproteinase-2 processing and tumor angiogenesis. J Biol Chem 2010;285:40039–49.
14. Chakraborty A, Boel NM, Edkins AL. HSP90 Interacts with the fibronectin N-terminal domains and increases matrix formation. Cells 2020;9:272.
15. McCready J, Sims JD, Chan D, Jay DG. Secretion of extracellular hsp90alpha via exosomes increases cancer cell motility: a role for plasminogen activation. BMC Cancer 2010;10:294.
16. McCready J, Wong DS, Burlison JA, Ying W, Jay DG. An impermeant ganetespib analog inhibits extracellular Hsp90-mediated cancer cell migration that involves lysyl oxidase 2-like protein. Cancers 2014;6:1031–46.
17. Chen WS, Chen CC, Chen LL, Lee CC, Huang TS. Secreted heat shock protein 90alpha (HSP90alpha) induces nuclear factor-kappaB-mediated TCF12 protein expression to down-regulate E-cadherin and to enhance colorectal cancer cell migration and invasion. J Biol Chem 2013;288:9001–10.
18. Gopal U, Bohonowych JE, Lema-Tome C, Liu A, Garrett-Mayer E, Wang B, et al A novel extracellular Hsp90 mediated co-receptor function for LRP1 regulates EphA2 dependent glioblastoma cell invasion. PLoS ONE 2011;6:e17649.
19. Hance MW, Dole K, Gopal U, Bohonowych JE, Jezierska-Drutel A, Neumann CA, et al Secreted Hsp90 is a novel regulator of the epithelial to mesenchymal transition (EMT) in prostate cancer. J Biol Chem 2012;287:37732–44.
20. Dong H, Zou M, Bhatia A, Jayaprakash P, Hofman F, Ying Q, et al Breast cancer MDA-MB-231 cells use secreted heat shock protein-90alpha (Hsp90alpha) to survive a hostile hypoxic environment. Sci Rep 2016;6:20605.
21. Tian Y, Wang C, Chen S, Liu J, Fu Y, Luo Y. Extracellular Hsp90alpha and clusterin synergistically promote breast cancer epithelial-to-mesenchymal transition and metastasis via LRP1. J Cell Sci 2019;132:jcs228213.
22. Thuringer D, Hammann A, Benikhlef N, Fourmaux E, Bouchot A, Wettstein G, et al Transactivation of the epidermal growth factor receptor by heat shock protein 90 via Toll-like receptor 4 contributes to the migration of glioblastoma cells. J Biol Chem 2011;286:3418–28.
23. Zou M, Bhatia A, Dong H, Jayaprakash P, Guo J, Sahu D, et al Evolutionarily conserved dual lysine motif determines the non-chaperone function of secreted Hsp90alpha in tumour progression. Oncogene 2017;36:2160–71.
24. Stellas D, Karameris A, Patsavoudi E. Monoclonal antibody 4C5 immunostains human melanomas and inhibits melanoma cell invasion and metastasis. Clin Cancer Res 2007;13:1831–8.

25. Tsutsumi S, Scroggins B, Koga F, Lee MJ, Trepel J, Felts S, et al A small-molecule cell-impermeant Hsp90 antagonist inhibits tumor cell motility and invasion. Oncogene 2008;27:2478–87.
26. Shirasu K, Lahaye T, Tan MW, Zhou F, Azevedo C, Schulze-Lefert P. A novel class of eukaryotic zinc-binding proteins is required for disease resistance signaling in barley and development in C. elegans. Cell 1999;99:355–66.
27. Hahn JS. Regulation of Nod1 by Hsp90 chaperone complex. FEBS Lett 2005;579:4513–9.
28. Gano JJ, Simon JA. A proteomic investigation of ligand-dependent HSP90 complexes reveals CHORDC1 as a novel ADP-dependent HSP90-interacting protein. Mol Cell Proteomics 2010;9:255–70.
29. Garcia-Ranea JA, Mirey G, Camonis J, Valencia A. p23 and HSP20/alpha-crystallin proteins define a conserved sequence domain present in other eukaryotic protein families. FEBS Lett 2002;529:162–7.
30. Ferretti R, Palumbo V, Di Savino A, Velasco S, Sbroggio M, Sportoletti P, et al Morgana/chp-1, a ROCK inhibitor involved in centrosome duplication and tumorigenesis. Dev Cell 2010;18:486–95.
31. Wu J, Luo S, Jiang H, Li H. Mammalian CHORD-containing protein 1 is a novel heat shock protein 90-interacting protein. FEBS Lett 2005;579:421–6.
32. Michowski W, Ferretti R, Wisniewska MB, Ambrozkiewicz M, Beresewicz M, Fusella F, et al Morgana/CHP-1 is a novel chaperone able to protect cells from stress. Biochim Biophys Acta 2010;1803:1043–9.
33. Fusella F, Ferretti R, Recupero D, Rocca S, Di Savino A, Tornillo G, et al Morgana acts as a proto-oncogene through inhibition of a ROCK–PTEN pathway. J Pathol 2014;234:152–63.
34. Fusella F, Secli L, Busso E, Krepelova A, Moiso E, Rocca S, et al The IKK/NF-kappaB signaling pathway requires Morgana to drive breast cancer metastasis. Nat Commun 2017;8:1636.
35. Di Savino A, Panuzzo C, Rocca S, Familiari U, Piazza R, Crivellaro S, et al Morgana acts as an oncosuppressor in chronic myeloid leukemia. Blood 2015;125:2245–53.
36. Feizi A, Banaei-Esfahani A, Nielsen J. HCSD: the human cancer secretome database. Database 2015;2015:bav051.
37. Tang X, Chang C, Guo J, Lincoln V, Liang C, Chen M, et al Tumour-secreted Hsp90alpha on external surface of exosomes mediates tumour—stromal cell communication via autocrine and paracrine mechanisms. Sci Rep 2019;9:15108.
38. Urabe F, Kosaka N, Sawa Y, Yamamoto Y, Ito K, Yamamoto T, et al miR-26a regulates extracellular vesicle secretion from prostate cancer cells via targeting SHC4, PFDN4, and CHORDC1. Sci Adv 2020;6:eaay3051.

39. Mamat U, Woodard RW, Wilke K, Souvignier C, Mead D, Steinmetz E, et al Endotoxin-free protein production—ClearColi technology. Nat Methods 2013;10:916.
40. Zhang G, Liu Z, Ding H, Zhou Y, Doan HA, Sin KWT, et al Tumor induces muscle wasting in mice through releasing extracellular Hsp70 and Hsp90. Nat Commun 2017;8:589.
41. Luo L, Wall AA, Tong SJ, Hung Y, Xiao Z, Tarique AA, et al TLR crosstalk activates LRP1 to recruit Rab8a and PI3Kgamma for suppression of inflammatory responses. Cell Rep 2018;24:3033–44.
42. Scott AM, Wolchok JD, Old LJ. Antibody therapy of cancer. Nat Rev Cancer 2012;12:278–87.
43. Redman JM, Hill EM, AlDeghaither D, Weiner LM. Mechanisms of action of therapeutic antibodies for cancer. Mol Immunol 2015;67:28–45.
44. Weiskopf K, Weissman IL. Macrophages are critical effectors of antibody therapies for cancer. mAbs 2015;7:303–10.
45. Weiss JM, Guerin MV, Regnier F, Renault G, Galy-Fauroux I, Vimeux L, et al The STING agonist DMXAA triggers a cooperation between T lymphocytes and myeloid cells that leads to tumor regression. Oncoimmunology 2017;6:e1346765.
46. Srivastava P. Roles of heat-shock proteins in innate and adaptive immunity. Nat Rev Immunol 2002;2:185–94.
47. Zhai E, Liang W, Lin Y, Huang L, He X, Cai S, et al HSP70/HSP90-organizing protein contributes to gastric cancer progression in an autocrine fashion and predicts poor survival in gastric cancer. Cell Physiol Biochem 2018;47:879–92.
48. El Hamidieh A, Grammatikakis N, Patsavoudi E. Cell surface Cdc37 participates in extracellular HSP90 mediated cancer cell invasion. PLoS ONE 2012;7:e42722.
49. Di Gioia M, Zanoni I. Toll-like receptor co-receptors as master regulators of the immune response. Mol Immunol 2015;63:143–52.
50. Azizi E, Carr AJ, Plitas G, Cornish AE, Konopacki C, Prabhakaran S, et al Single-cell map of diverse immune phenotypes in the breast tumor microenvironment. Cell 2018;174:1293–308.

Graphical Abstract

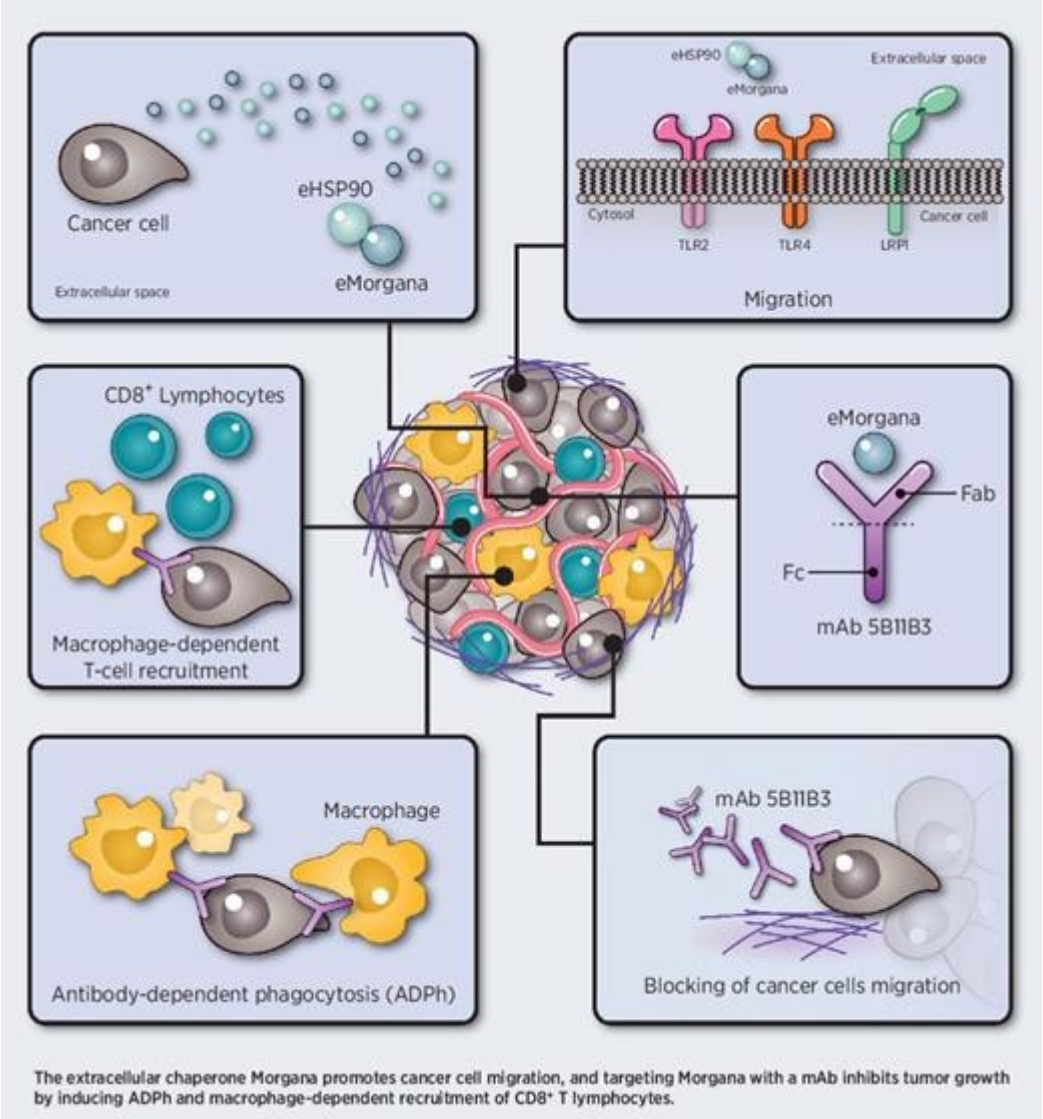

The extracellular chaperone Morgana promotes cancer cell migration, and targeting Morgana with a mAb inhibits tumor growth by inducing ADPh and macrophage-dependent recruitment of CD8+ T lymphocytes.

Figure 1

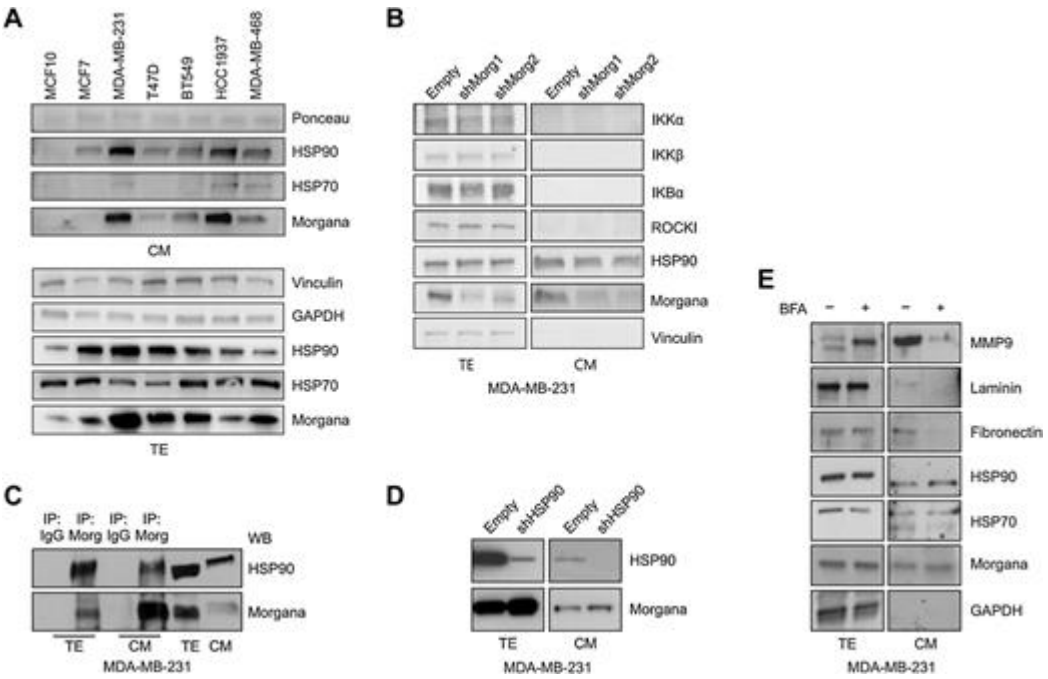

Morgana is secreted by cancer cells through an uncanonical pathway. **A**, Western blot analysis of Morgana expression in the total extract (TE) and in conditioned medium (CM) of human breast normal and cancer cell lines. Extracellular HSP70 and HSP90 in the CM were used as positive controls and the Ponceau staining as loading control. Vinculin and GADPH were used as loading control in TE. **B**, Western blot analysis of TE and CM of MDA-MB-231 infected with an empty vector or with two different shRNAs against Morgana (shMorg1 and shMorg2). Proteins known to interact with Morgana in the cytoplasm (IκB, IKKα, IKKβ, and ROCKI) were not detectable in the CM. HSP90 and vinculin were used as positive and negative control, respectively. **C**, Coimmunoprecipitation experiments of Morgana and HSP90 from MDA-MB-231 TE and CM. Unrelated IgGs were used as control. **D**, TE and CM from MDA-MB-231 empty and silenced for HSP90 (shHSP90) were analyzed by Western blotting for the presence of Morgana. **E**, Western blot analysis of TE and CM of MDA-MB-231 cells treated with brefeldin A (BFA; 10 μg mL^{-1}) for 5 hours. Proteins secreted through the ER–Golgi pathway (MMP9, laminin, and fibronectin) were used as controls. Proteins known to be secreted through unconventional pathways (HSP70 and HSP90) were also analyzed. GAPDH was used as loading and negative control.

Figure 2

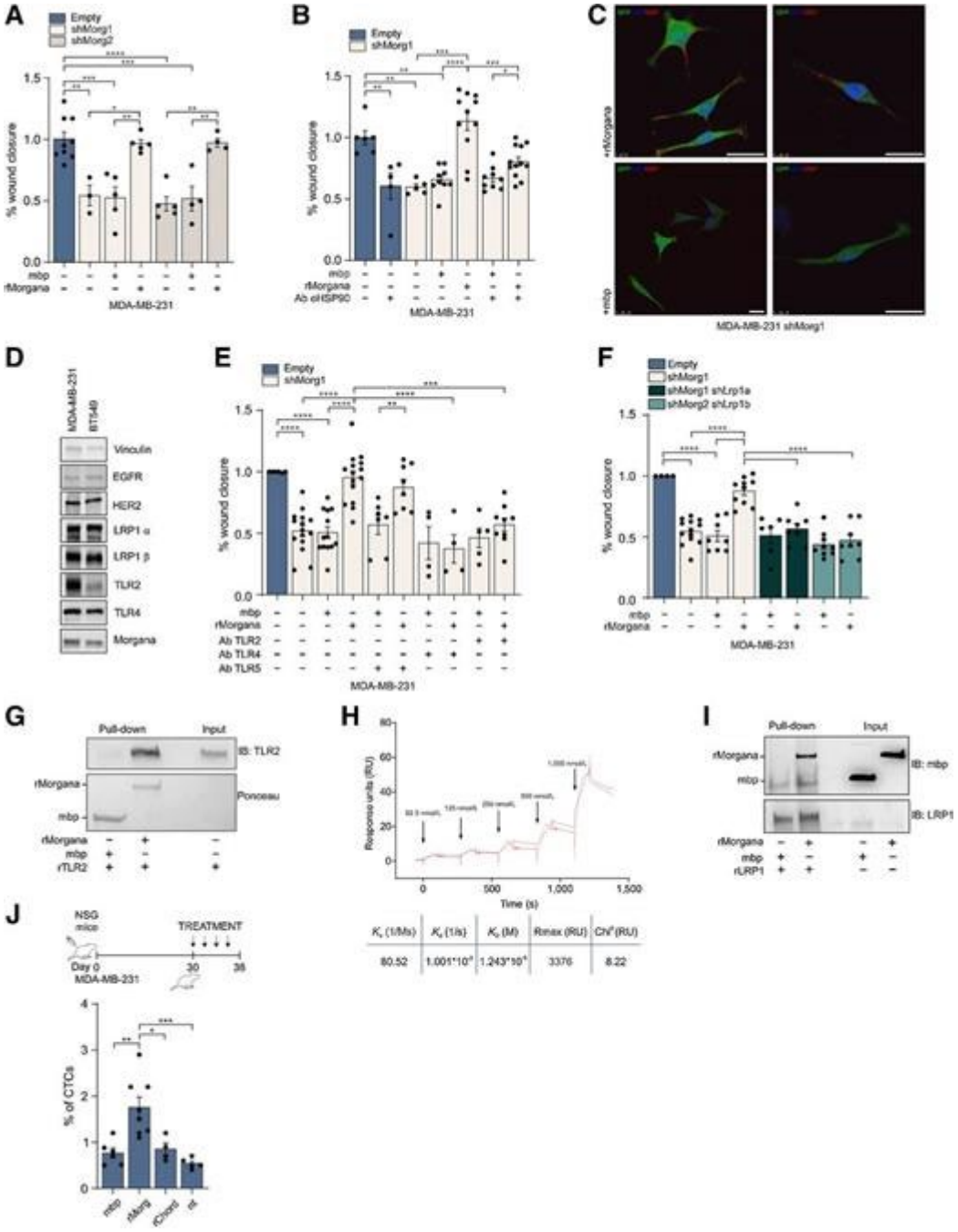

Extracellular Morgana induces cancer cell migration through TLR2, TLR4, and LRP1 receptors. **A**, MDA-MB-231 empty and shMorg1/2 cells were treated or not with 0.1 µmol/L of mbp or mbp-Morgana (rMorgana), wounded, and images were captured immediately and 24 hours later. Data are presented as median values ± SEM; n ≥ 3 experiments. One-way ANOVA tests with Bonferroni *post hoc* test were performed to obtain *P* values. **B**, MDA-MB-231 empty and shMorg1/2 cells were treated or not with 0.1 µmol/L of mbp or rMorgana in combination or not with a neutralizing antibody against HSP90 (100 ng mL^{-1}). After wounding, images were captured immediately and 24

hours later. Data are presented as median values ± SEM; n ≥ 5 experiments. One-way ANOVA tests with Bonferroni *post hoc* test were performed to obtain *P* values. **C**, Immunofluorescence of MDA-MB-231 shMorg1 cells treated with mbp or rMorgana (0.1 μmol/L). Cells were not permeabilized and stained with an anti-mbp antibody (red) and nuclei were stained with DAPI (blue). White bars, 25 μm. D, The expression of EGFR, HER2, LRP1 (α and β subunits), TLR2, TLR4, and Morgana was analyzed by Western blot in MDA-MB-231 and BT549. **E**, MDA-MB-231 shMorg1 cells treated with 0.1 μmol/L of mbp or rMorgana alone or in combination with a monoclonal antibody against TLR2 (30 ng mL^{-1}), TLR4 (100 ng mL^{-1}), TLR5 (100 ng mL–1) were wounded, and images were captured immediately and 24 hours after wounding. Data are presented as median values ± SEM; n ≥ 4 experiments. One-way ANOVA tests with Bonferroni *post hoc* test were performed to obtain *P* values. **F**, MDA-MB-231 empty, shMorg1/2, and silenced for both Morgana and LRP1 (shMorg1 shLrp1a and shMorg2 shLrp1b) were treated or not with 0.1 μmol/L of mbp or rMorgana. After wounding, images were captured immediately and 24 hours later. Data are presented as median values ± SEM; n ≥ 4 experiments. One-way ANOVA tests with Bonferroni *post hoc* tests were performed to obtain P values. **G**, Pull down experiments showing the ability of rMorgana to bind directly to the extracellular portion of recombinant TLR2 (rTLR2). The interaction has been tested in unconditioned medium. **H**, Surface plasmon resonance analysis of Morgana–TLR2 interaction. Increasing concentrations of rMorgana were injected over a TLR2-coated chip. Morgana binds to TLR2 with an equilibrium dissociation constant (KD) of 12.43 μmol/L. K_a, association rate constant; *M*, molarity; *s*, seconds; K_d, dissociation rate constant; K_D, equilibrium dissociation constant; R_{max}, maximum response; *RU*, response units; χ^2, average squared residual. **I**, Pull down experiments testing the ability of a recombinant protein containing the LRP1 cluster II domain (rLRP1) to interact with rMorgana. The interaction was tested in CM. J, NSG mice carrying MDA-MB-231–derived tumors (25 mm^3) were subjected to intratumor injections of rMorgana, rChord (N-terminal Morgana), or mbp as control (100 μg/mouse/injection, every other day). The graph indicates the percentage of MDA-MB-231 GFP+ circulating tumor cells (CTC), in the blood of mice after four treatments. Data are presented as median values ± SEM; n ≥ 4 mice per group. One-way ANOVA tests with Bonferroni *post hoc* test were performed to obtain *P* values. *, $P < 0.05$; **, $P < 0.005$; ***, $P < 0.0005$; ****, $P < 0.0001$.

Figure 3

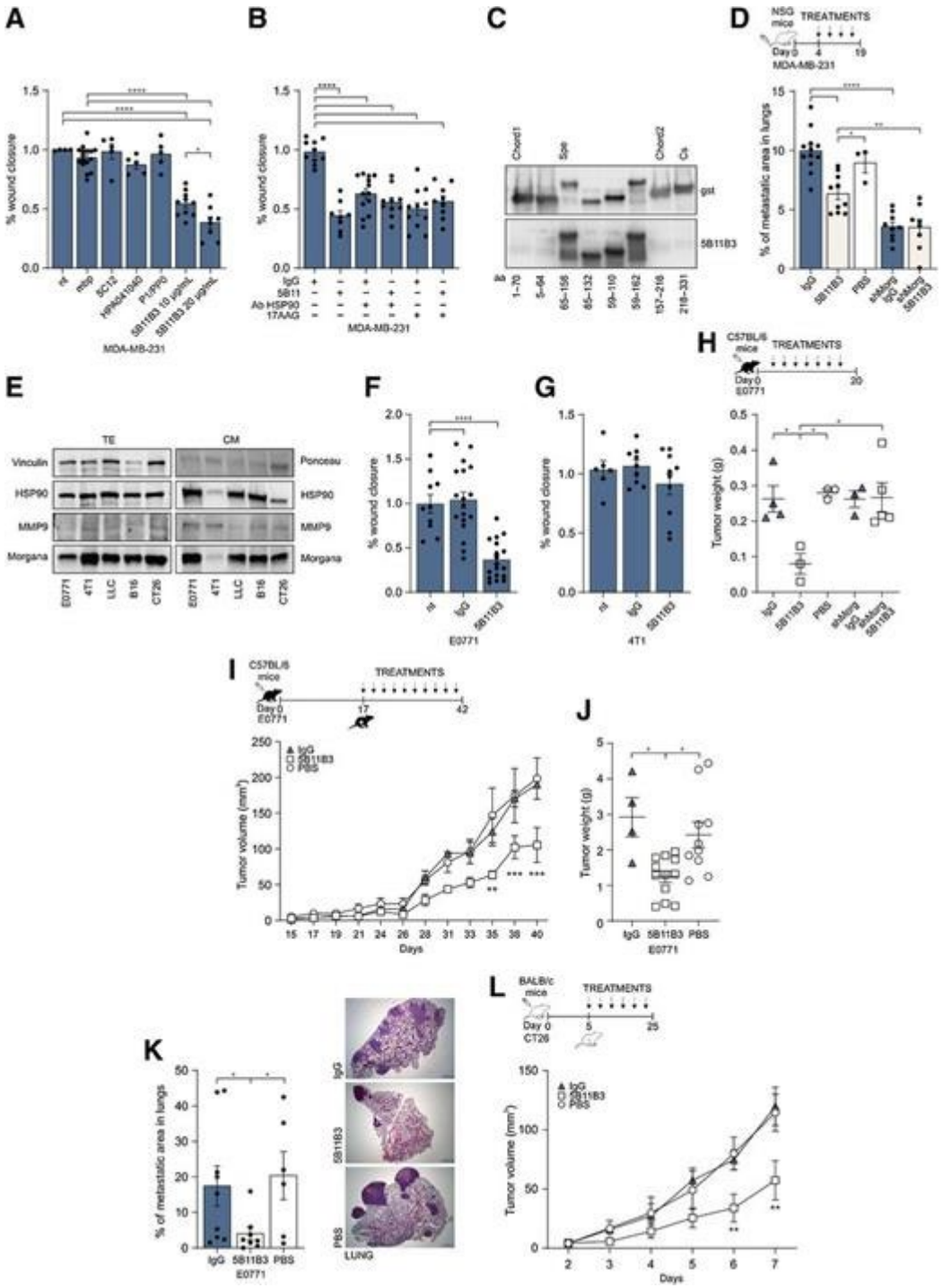

The anti-Morgana mAb 5B11B3 impairs tumor growth and metastasis formation. **A**, MDA-MB-231 cells were treated with different antibodies against Morgana (10 µg mL^{-1}), wounded, and images captured immediately and 24 hours after wounding. An anti-mbp antibody was used as control IgG. Data are presented as median values ± SEM; n ≥ 4 experiments. One-way ANOVA tests with Bonferroni *post hoc* test were performed to obtain *P* values. **B**, MDA-MB-231 cells were treated

with mAb 5B11B3 against Morgana or control IgG (15 μg mL^{-1}) in combination or not with the inhibition of HSP90 (blocking mAb, 100 ng mL^{-1} or 17AAG, 1 μmol/L). Cells were wounded and images captured immediately and after 24 hours. Data are presented as median values ± SEM; n ≥ 8 experiments. One-way ANOVA tests with Bonferroni *post hoc* test were performed to obtain *P* values. **C**, Different pieces of Morgana fused to gst were analyzed by Western blotting to identify the portion bound by the mAb 5B11B3. Gst was used as negative control. **D**, Lung metastatic burden of NSG mice injected intravenously with 5×10^5 MDA-MB-231 or MDA-MB-231 downregulated for Morgana (shMorg) and treated with mAb 5B11B3 or IgG as control (100 μg, intravenous injection, twice a week, for a total of four treatments). Data are presented as median values ± SEM; n ≥ 3 lung lobes. One-way ANOVA tests with Bonferroni *post hoc* test were performed to obtain *P* values. **E**, Western blot analysis of Morgana, HSP90, and MMP9 on TE and CM of murine cancer cell lines. Vinculin and Ponceau staining were used as loading controls in TE and CM, respectively. F and G, E0771 (F) and 4T1 (G) cells were treated with mAb 5B11B3 or control IgG (15 μg mL^{-1}), wounded, and images captured immediately and 24 hours after wounding. Data are presented as median values ± SEM; n ≥ 10 experiments for E0771 and n ≥ 6 experiments for 4T1 cells. One-way ANOVA tests with Bonferroni *post hoc* test were performed to obtain *P* values. **H**, Tumor weight of C57BL/6 mice inoculated subcutaneously with 2×10^5 E0771 or E0771 shMorg and treated with mAb 5B11B3 or with control IgG (100 μg, intravenous injection, three times per week). Animals were sacrificed after 20 days. Data are presented as median values ± SEM; n ≥ 3 mice per group. One-way ANOVA tests with Bonferroni *post hoc* test were performed to obtain *P* values. I–K, Tumor volume (I), tumor weight (J), and lung metastatic burden (K) of C57BL/6 mice inoculated subcutaneously with 2×10^5 E0771 cells and sacrificed at 42 days. After primary tumor development (size around 15 mm^3), animals were treated with mAb 5B11B3 or control IgG (100 μg, intravenous injection, three times per week). Representative H&E-stained sections of mouse lungs are also shown; bar, 250 μm. I and J, n ≥ 4 mice. Two-way ANOVA tests with Bonferroni *post hoc* test and one-way ANOVA with Bonferroni *post hoc* test were performed to obtain *P* values, respectively. **K**, n ≥ 6 lung lobes. One-way ANOVA with the Fisher LSD test *post hoc* test was performed to obtain *P* values. **L**, Tumor volume of BALB/c mice inoculated subcutaneously with 2×10^5 CT26 and treated with mAb 5B11B3 or control IgG (100 μg, intravenous injection, three times per week). Animals were sacrificed after 25 days. n ≥ 3 mice. Two-way ANOVA test with the Bonferroni *post hoc* test was performed to obtain *P* values. *, $P < 0.05$; **, $P < 0.005$; ****, $P < 0.0001$.

Figure 4

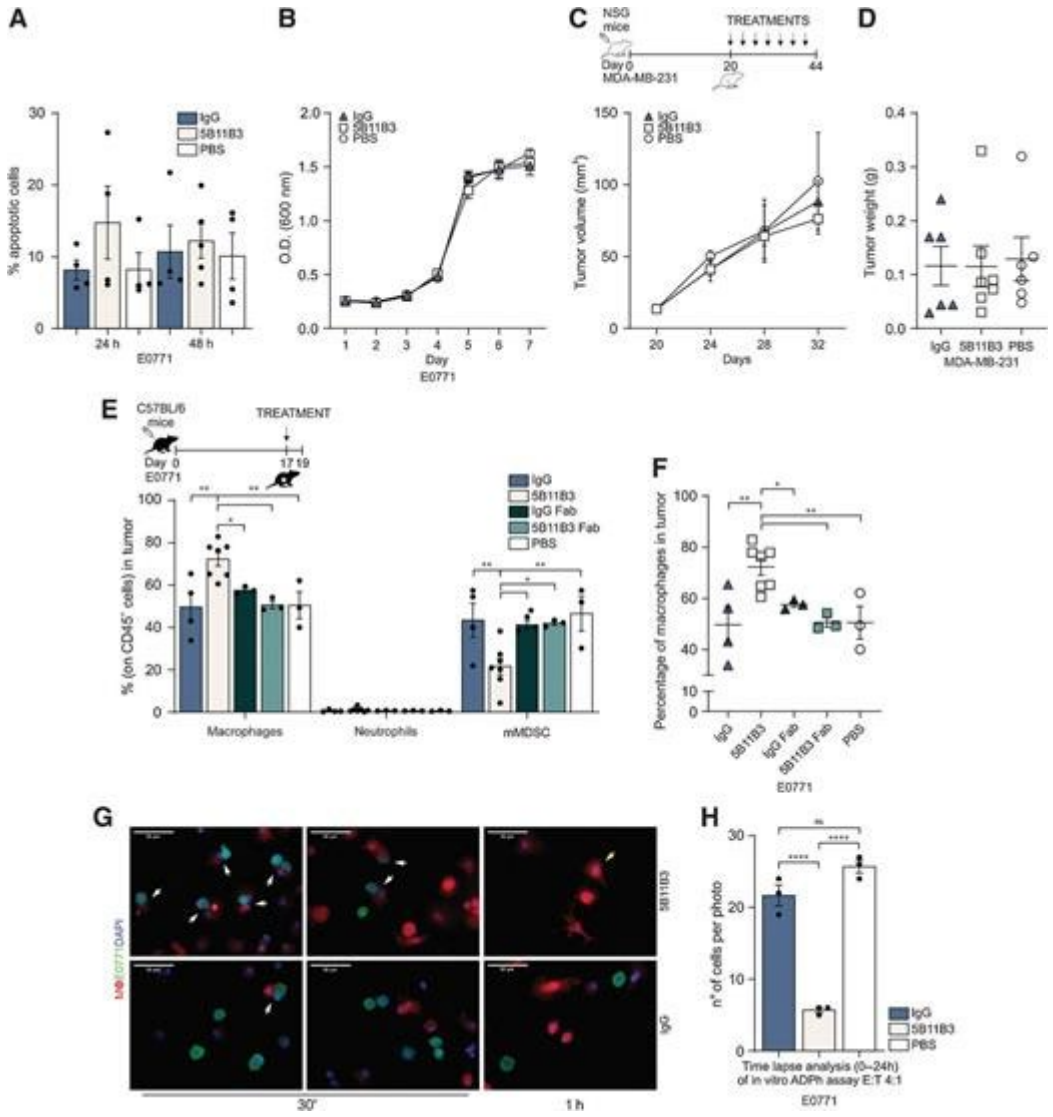

mAb 5B11B3 recruits macrophages in the tumor. **A and B**, Apoptosis (**A**) and proliferation (**B**) of E0771 cells treated or not with mAb 5B11B3 or control IgG (15 µg mL^{-1}). Data are presented as median values ± SEM; n ≥ 4 experiments. **C and D**, Tumor volume (**C**) and tumor weight (**D**) of NSG immunocompromised mice inoculated subcutaneously with 1 × 10^6 MDA-MB-231 cells and treated with mAb 5B11B3 or control IgG (100 µg, intravenous injection, three times per week). After 1 month, mice were sacrificed. Data are presented as median values ± SEM; n ≥ 6 mice per group. **E and F**, The percentages of immune cells (gated on CD45+ cells; **E**) and of macrophages (**F**) were assessed by flow cytometry in E0771-derived tumors (size around 15 mm^3) from C57BL/6 mice treated with mAb 5B11B3, IgG, 5B11B3 Fab, or IgG Fab once (100 µg, intravenous injection) and sacrificed 24 hours later. Data are presented as median values ± SEM; n ≥ 3 mice. One-way ANOVA test with the Fisher LSD test *post hoc* test was performed to obtain *P* values. **G**, Representative fluorescence images of cocultures of C57BL/6 BMDMs (Orange CMRA Dye) and

E0771 cells (Green CMFDA Dye) in an E:T ratio of 4:1 in presence of mAb 5B11B3 or control IgG (10 µg) at 30′ and 1 hour. DAPI was used to stain nuclei. White arrows indicate BMDMs in proximity to E0771 cells. The yellow arrow shows the presence of green spots inside a BMDM, probably the remains of a green tumor cell engulfed by the macrophage. White bar, 50 µm. **H**, ADPh: quantification of E0771 cancer cells after 24 hours of coculturing experiments with C57BL/6 BMDMs (E:T ratio 4:1) in presence of 10 µg of mAb 5B11B3 or control IgG. Data are presented as median values ± SEM; n = 3 experiments. One-way ANOVA tests with Bonferroni *post hoc* test were performed to obtain *P* values. *, $P < 0.05$; **, $P < 0.005$; ****, $P < 0.0001$; ns, nonsignificant.

Figure 5

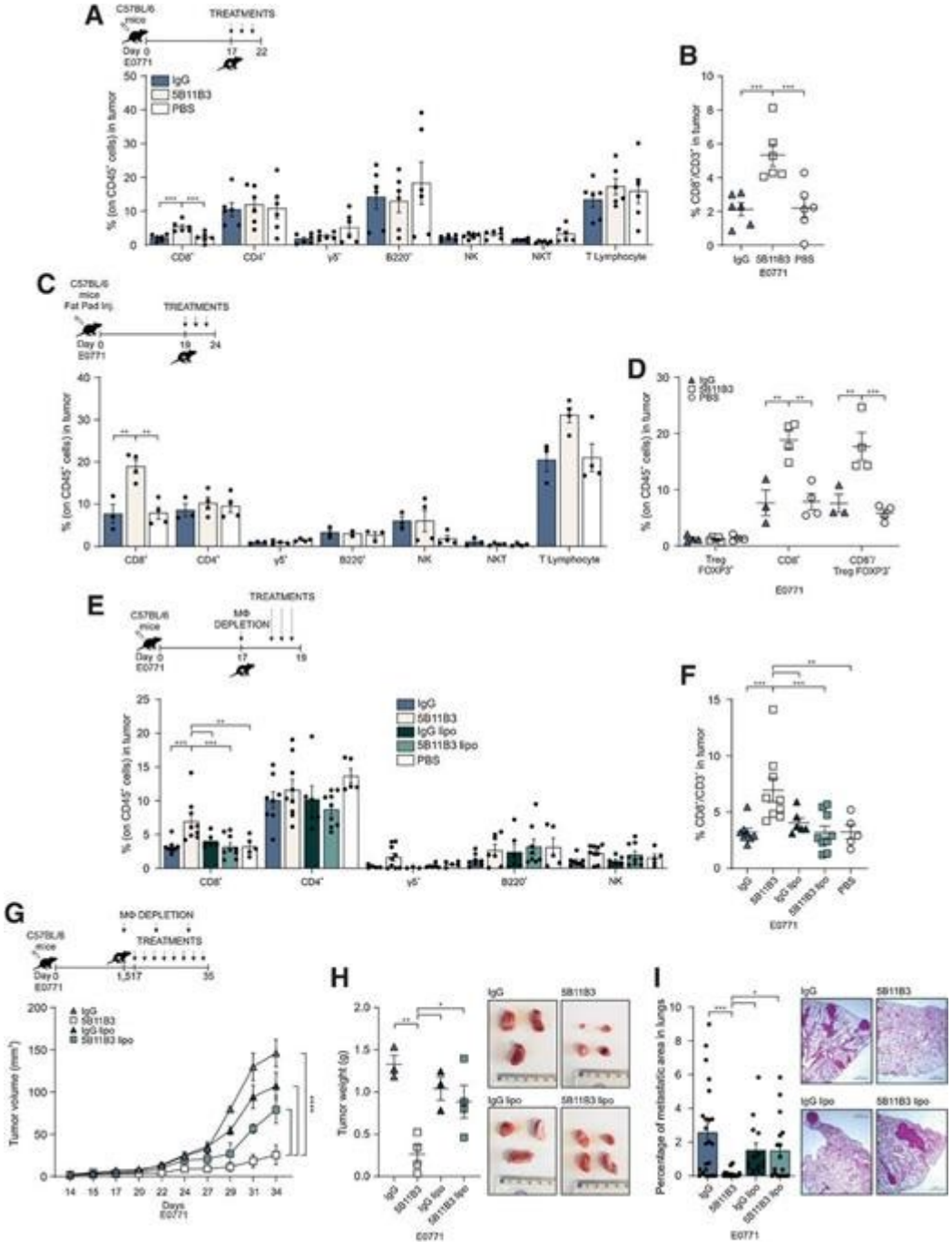

mAb 5B11B3-recruited macrophages attract CD8⁺ T lymphocytes at the tumor site. **A and B**, Percentage of immune cells (gated on CD45⁺ cells; **A**) and percentage of CD8⁺ T lymphocytes (**B**) in tumors of C57BL/6 mice carrying E0771-derived tumors. After primary tumor development (size around 15 mm^3), animals were treated with mAb 5B11B3, control IgG, or PBS three times (100 µg, intravenous injection) and sacrificed. Data are presented as median values ± SEM; n = 6 mice per group. One-way ANOVA test with Fisher LSD test *post hoc* test was performed to obtain *P* values. **C and D**, Percentage of immune cells (gated on CD45⁺ cells; **C**) and percentage of Treg FOXP3⁺,

$CD8^+$ T lymphocytes and ratio of $CD8^+$ T lymphocytes/Treg $FOXP3^+$ (D) in E0771-derived fat pad tumors. After fat pad tumor development, animals were treated with mAb 5B11B3, control IgG, or PBS three times (100 µg, intravenous injection) and sacrificed. Data are presented as median values ± SEM; n ≥ 3 mice per group. One-way ANOVA test with Fisher LSD test *post hoc* test was performed to obtain *P* values. **E and F**, Percentage of immune cells (gated on $CD45^+$ cells; **E**) and percentage of $CD8^+$ T lymphocytes (F) in E0771-derived tumors. After primary tumor development (size around 15 mm^3), animals were treated with clodronate liposomes (lipo) in PBS (100 µg per 10 gr/mouse) and after 4 days, mice were treated with mAb 5B11B3 or IgG (100 µg, intravenous injection, every other day) three times and sacrificed. Data are presented as median values ± SEM; n ≥ 3 mice per group. One-way ANOVA test with Fisher LSD test *post hoc* test was performed to obtain *P* values. **G–I**, Tumor volume, tumor weight (**H**), and lung metastatic burden (**I**) of C57BL/6 mice inoculated subcutaneously with 2×10^5 E0771 cells and sacrificed at 35 days. At 15 days, animals were treated or not with clodronate liposomes (lipo) in PBS (100 µg per 10 gr/mouse) and at 17 days (primary tumor size around 15 mm^3), mice were treated with mAb 5B11B3 or IgG (100 µg, intravenous injection, three times per week). Photos of tumors after animal sacrifice and H&E-stained sections of mouse lungs; black bar, 200 µm. In G and H, n ≥ 3 mice per group. Respectively, two-way ANOVA test with Bonferroni *post hoc* test and one-way ANOVA with Bonferroni *post hoc* test were performed to obtain *P* values. I, n ≥ 15 lung lobes. One-way ANOVA with Fisher LSD test *post hoc* test was performed to obtain *P* values. *, $P < 0.05$; **, $P < 0.005$; ***, $P < 0.001$; ****, $P < 0001$.

Supplementary Figures

Supplementary Fig. S1

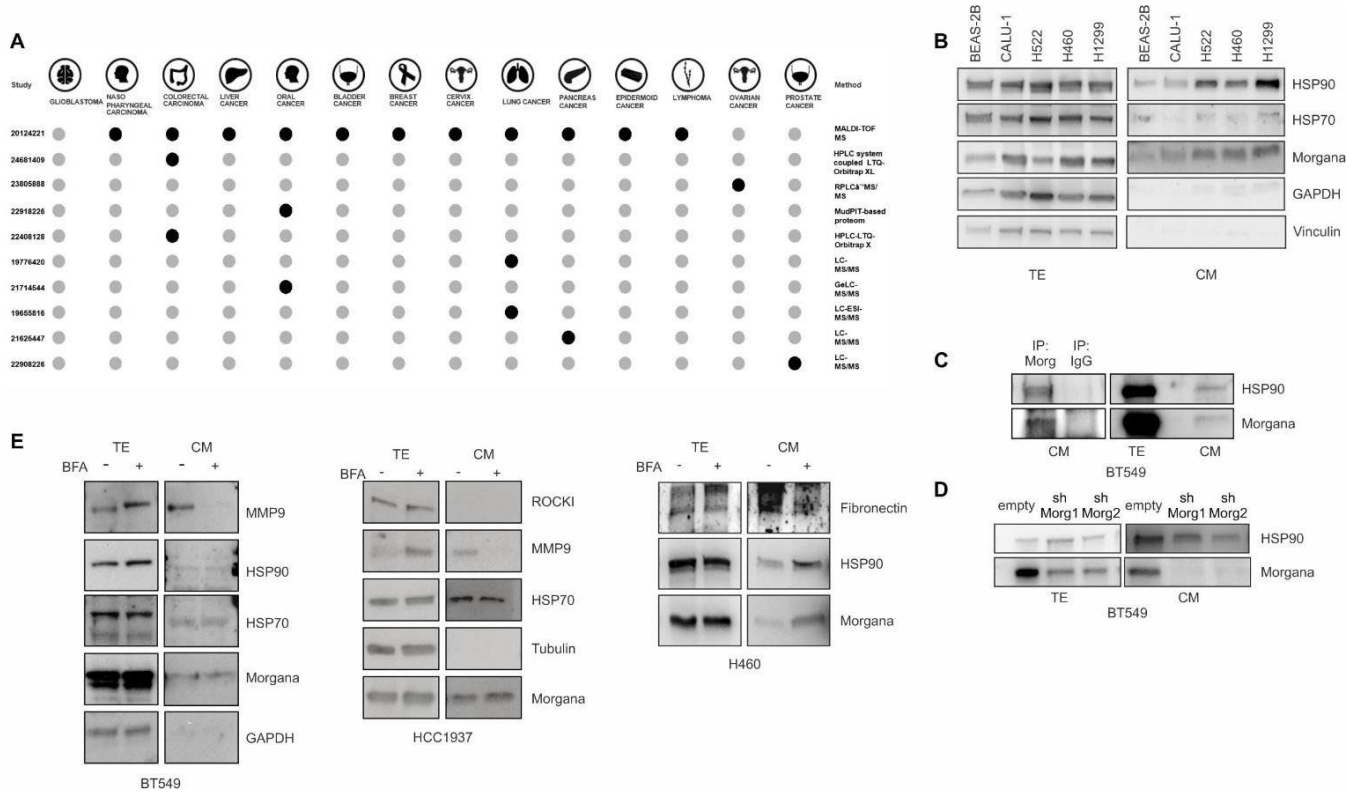

Supplementary Fig. S1. Morgana is secreted by cancer cells. (**A**) Data from Human Cancer Secretome Database indicated that Morgana is secreted by different types of cancer cells. Dark dots represent experiments in which Morgana has been identified in cancer cell secretomes. (**B**) Western blot analysis to detect Morgana, HSP70 and HSP90 in the total extracts (TE) and in the conditioned media (CM) of human lung normal and cancer cell lines. GAPDH and Vinculin were used as loading and negative control for TE and CM, respectively. (**C**) Co-immunoprecipitation experiments of Morgana and HSP90 in BT549 cell CM. An unrelated IgG was used as control. (**D**) BT549 empty and downregulated for Morgana (shMorg1/2) were analyzed by Western blotting to detect HSP90. (**E**) Western blot analysis of TE and CM of BT549, HCC1937 and H460 cells, treated with Brefeldin A (10 $\mu g\ ml^{-1}$) for 5 h. Proteins secreted through the conventional ER-Golgi pathway (MMP9 and Fibronectin) were used as control for the treatment. Proteins known to be secreted through

unconventional pathways (HSP70 and HSP90) were also analyzed. GAPDH and Tubulin were used as loading and negative control for TE and CM, respectively.

Supplementary Fig. S2

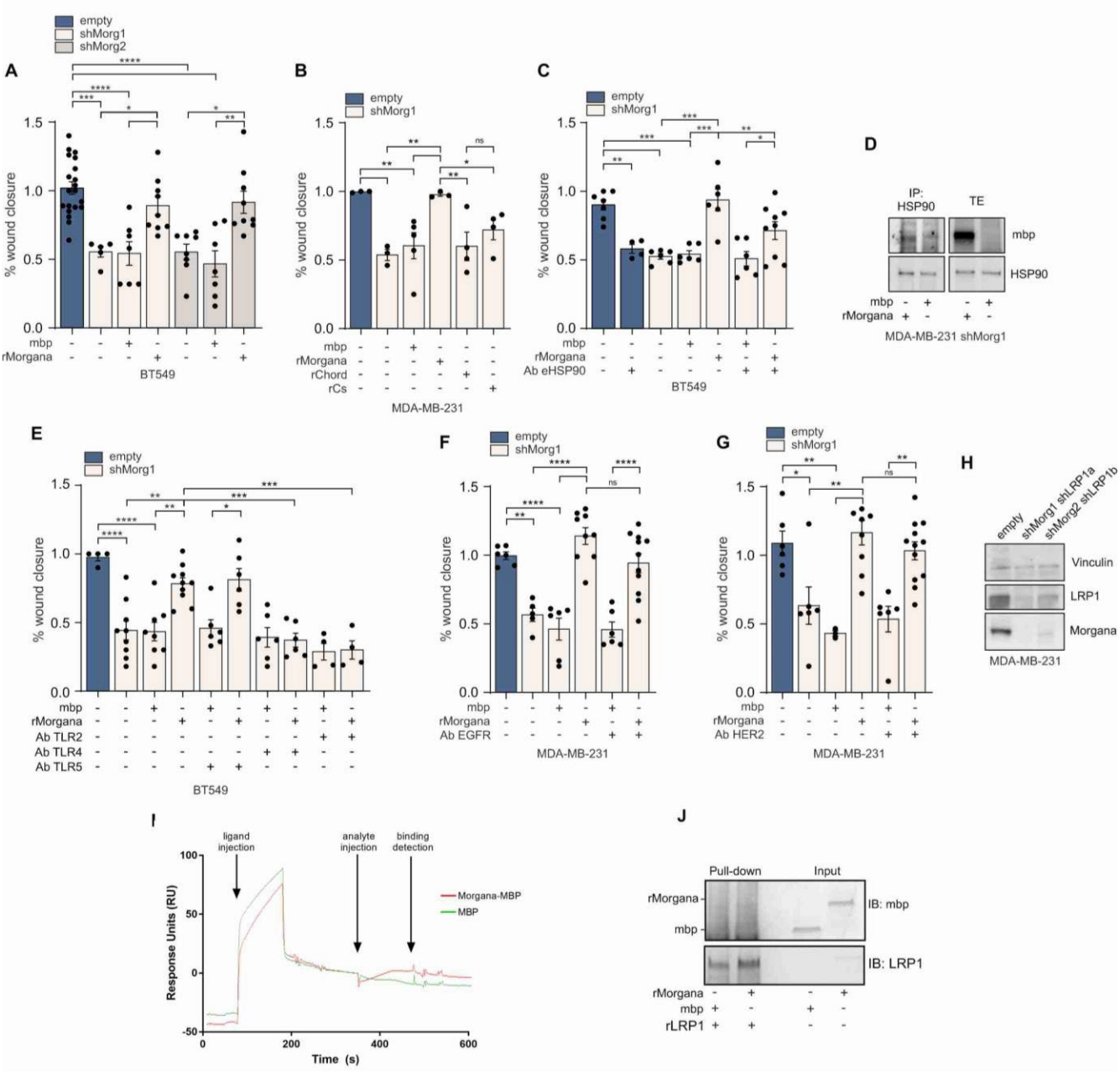

Supplementary Fig. S2. Extracellular Morgana induces migration in cancer cells. (**A**) BT549 empty and shMorg1/2 cells were treated or not with 0.1 μM of mbp or mbp-Morgana (rMorgana). Images were captured immediately after wounding and 24 h later. Bars represent the percentage of wound closure. Data are presented as median values ± SEM; n ≥ 5 experiments. One-way ANOVA tests

with Bonferroni post hoc test were performed to obtain P values. (**B**) MDA-MB-231 shMorg1 cells (treated with 0.1 μM of mbp, rMorgana, rChord or rCs) were wounded and images captured immediately and 24 h after wounding. Data are presented as median values ± SEM; n ≥ 3 experiments. One-way ANOVA tests with Bonferroni post hoc test were performed to obtain P values. (C) BT549 empty and shMorg1/2 cells were treated or not with 0.1 μM of mbp or rMorgana in combination or not with an HSP90-neutralizing antibody (100 ng ml^{-1}). Images were captured immediately after wounding and 24 h later. Data are presented as median values ± SEM; n ≥ 4 experiments. One-way ANOVA tests with Bonferroni post hoc test were performed to obtain P values. (D) MDA-MB-231 shMorg cells treated with 0.1 μM of mbp or rMorgana (2 h, 4°C) were washed and exposed to DTSSP cross-linking and lysed. Protein extracts were subjected to immunoprecipitation using anti-HSP90 antibodies. Total extracts (TE) were analyzed for the presence of rMorgana by Western blot. (**E**) BT549 shMorg1 cells, treated with 0.1 μM of mbp or rMorgana alone or in combination with a monoclonal antibody against TLR2 (30 ng ml^{-1}), TLR4 (100 ng ml^{-1}) or TLR5 (100 ng ml^{-1}) were wounded and images captured immediately and 24 h after wounding. Data are presented as median values ± SEM; n ≥ 4 experiments. One-way ANOVA tests with Bonferroni post hoc test were performed to obtain P values. (**F-G**) MDA-MB-231 shMorg1 cells, treated with 0.1 μM of mbp or rMorgana alone or in combination with a monoclonal antibody against EGFR (1 μM) or HER2 (1 μg ml^{-1}) were wounded and images captured immediately and 24 h after wounding. Data are presented as median values ± SEM; n ≥ 3 experiments. One-way ANOVA tests with Bonferroni post hoc test were performed to obtain P values. (**H**) Western blot analysis of MDA-MB-231 infected with an empty vector or with two different shRNAs against LRP1 and Morgana (shMorg1shLRP1a and shMorg2shLRP1b). Vinculin was used as loading control. (I) Upon TLR2 (ligand) immobilization onto a CM5 sensor chip through anti-His antibody, 1 μM of mbp-Morgana or mbp alone (analytes) were injected. A specific binding was detected only when mbp-Morgana fusion protein was used (120 s from analyte injection). (J) Pull down experiments testing the ability of a recombinant protein

containing the LRP1 cluster II domain to interact directly with rMorgana. The interaction has been tested in unconditioned medium (*$p < 0.05$; **$p < 0.005$; ***$p < 0.0005$; ****$p < 0.0001$).

Supplementary Fig. S3

Figure S3

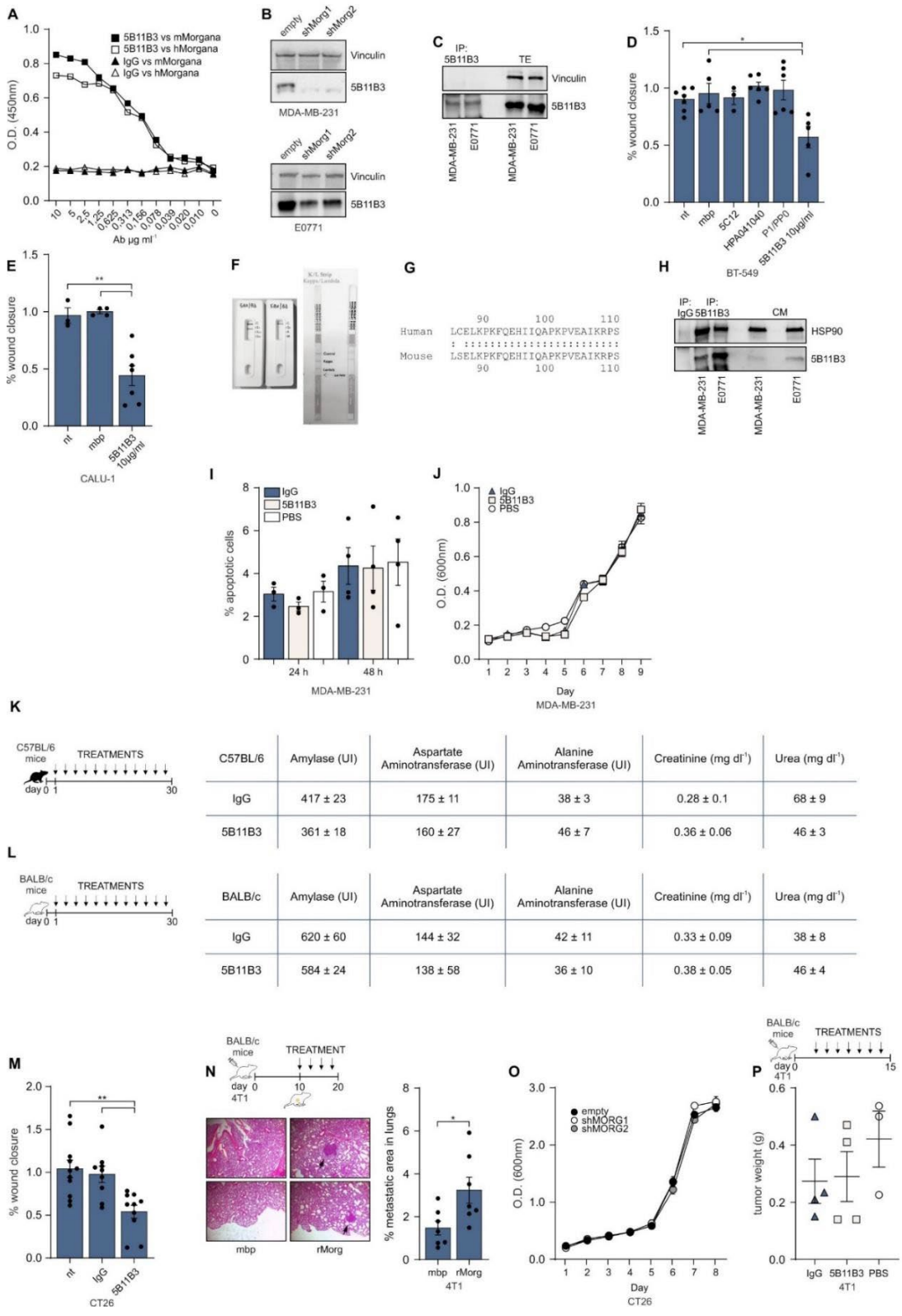

C57BL/6	Amylase (UI)	Aspartate Aminotransferase (UI)	Alanine Aminotransferase (UI)	Creatinine (mg dl^{-1})	Urea (mg dl^{-1})
IgG	417 ± 23	175 ± 11	38 ± 3	0.28 ± 0.1	68 ± 9
5B11B3	361 ± 18	160 ± 27	46 ± 7	0.36 ± 0.06	46 ± 3

BALB/c	Amylase (UI)	Aspartate Aminotransferase (UI)	Alanine Aminotransferase (UI)	Creatinine (mg dl^{-1})	Urea (mg dl^{-1})
IgG	620 ± 60	144 ± 32	42 ± 11	0.33 ± 0.09	38 ± 8
5B11B3	584 ± 24	138 ± 58	36 ± 10	0.38 ± 0.05	46 ± 4

Supplementary Fig. S3. Characterization of mAb 5B11B3. (**A**) ELISA assays with serial dilution of mAb 5B11B3 or control IgG on human and mouse rMorgana proteins (10 μg ml^{-1}). (**B**) Western blot analysis with mAb 5B11B3 of MDA-MB-231 and E0771 empty or shMorg1 and shMorg2. Vinculin was used as loading control. (**C**) mAb 5B11B3 was used in an immunoprecipitation experiment from MDA-MB-231 and E0771 total extracts. Western blot analysis was performed using mAb 5B11B3 and Vinculin. (**D**) BT549 cells were treated with different antibodies against Morgana (10 μg ml^{-1}), wounded and images were captured immediately and 24 h later. An antibody against mbp was used as negative control. Data are presented as median values ± SEM; n ≥ 3 experiments. One-way ANOVA tests with Bonferroni post hoc test were performed to obtain P values. (**E**) CALU-1 cells were treated with mAb 5B11B3 (10 μg ml^{-1}), wounded and images were captured immediately and 24 h after wounding. An anti-mbp antibody was used as negative control. Data are presented as median values ± SEM; n ≥ 3 experiments. One-way ANOVA tests with Bonferroni post hoc test were performed to obtain P values. (**F**) Characterization of mAb 5B11B3 isotype and light chains. (**G**) Comparison of the amino acidic sequence of human and mouse Morgana from amino acid 85 to 110. (**H**) mAb 5B11B3 was used in an immunoprecipitation experiment from MDA-MB-231 and E0771 CM. Western blot analysis was performed using HSP90 and mAb 5B11B3. (**I**) Percentage of apoptotic MDA-MB-231 cells assessed by annexin V and propidium iodide staining at 24 and 48 h after treatment with control IgG or mAb 5B11B3 (10 μg ml^{-1}). Data are presented as median values ± SEM; n ≥ 3 experiments. (**J**) Proliferation assay on MDA-MB-231 cells treated with control IgG or mAb 5B11B3 (10 μg ml^{-1}). Data are presented as median values ± SEM; n ≥ 3 experiments. (**K-L**) Analysis of blood of C57BL/6 and BALB/c mice treated with mAb 5B11B3 or control IgG (100 μg, IV injection, 3 times per week). (**M**) CT26 cells were treated with mAb 5B11B3 or control IgG (10 μg ml^{-1}), wounded and images captured immediately and 24 h after wounding. Data are presented as median values ± SEM; n ≥ 9 experiments. One-way ANOVA tests with Bonferroni post hoc test were performed to obtain P values. (**N**) Lung metastatic burden of BALB/c mice injected with 1 x 10^5 4T1 and treated with intratumoral injection of rMorgana or mbp as control (100 μg, 4 injections, 2 times per week). Black arrow indicate

micrometastasis. Data are presented as median values ± SEM; n ≥ 7 lung lobes. One-way ANOVA tests with Fisher's LSD test post hoc were performed to obtain P values. (**O**) Proliferation assay on CT26 empty or shMorg1 and shMorg2 cells. Data are presented as median values ± SEM; n ≥ 3 experiments. (**P**) Tumor weight of BALB/c mice subcutaneously inoculated with 1 x 10^5 4T1 cells and treated with mAb 5B11B3 or control IgG (100 μg, IV injection, 3 times per week). Animals were sacrificed after 15 days. Data are presented as median values ± SEM; n ≥ 3 mice per group (*$p < 0.05$; **$p < 0.005$).

Supplementary Fig. S4

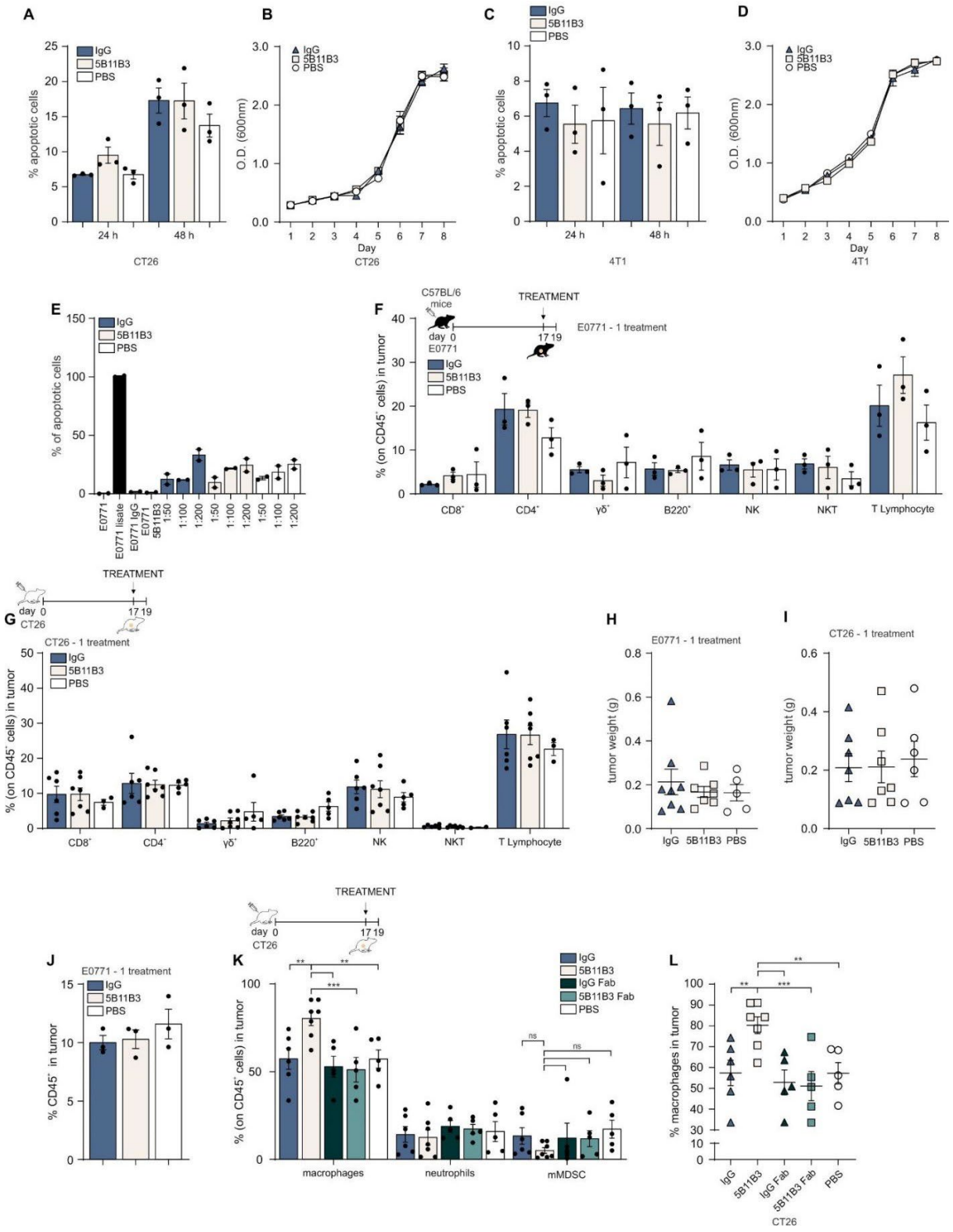

Supplementary Fig. S4. mAb 5B11B3 recruits macrophages in the primary tumor. (**A**) Percentage of apoptotic CT26 cells assessed by annexin V and propidium iodide staining at 24 and 48 h after treatment with control IgG or mAb 5B11B3 (10 μg ml^{-1}). Data are presented as median values ± SEM; n = 3 experiments. **(B)** Proliferation assay on CT26 cells treated with control IgG or mAb 5B11B3 (10 μg ml^{-1}) Data are presented as median values ± SEM; n = 3 experiments. (**C**) Percentage of apoptotic 4T1 cells assessed by annexin V and propidium iodide staining at 24 and 48 h after treatment with control IgG or mAb 5B11B3 (10 μg ml^{-1}). Data are presented as median values ± SEM; n = 3 experiments. **(D)** Proliferation assay on 4T1 cells treated with control IgG or mAb 5B11B3 (10 μg ml^{-1}). Data are presented as median values ± SEM; n = 3 experiments. (**E**) ADCC: percentage of E0771 apoptotic cells after co-culture of E0771 cells with splenocytes from C57BL/6 mice using 3 different E:T ratios (50:1, 100:1 and 200:1) in the presence of the mAb 5B11B3, control IgG (10 μg) or vehicle (PBS). (**F-J**) C57BL/6 mice or BALB/c mice subcutaneously inoculated respectively with 2 x 10^5 E0771 or 2 x 10^5 CT26 and after tumor growth, treated with mAb 5B11B3, IgG or vehicle (PBS) (100 μg, IV injection) and sacrificed after 24 h. (**F-G**) Lymphoid immune composition of the primary tumor, (**H-I**) tumor weight, (**J**) identification of $CD45^+$ cells in E0771-derived tumors. (**K-L**) BALB/c mice inoculated subcutaneously with 2 x 10^5 CT26. After primary tumor development (size around 15 mm^3), animals were treated with mAb 5B11B3, control IgG, 5B11B3 Fab, control IgG Fab or vehicle (PBS) one time (100 μg, IV injection) and sacrificed after 24 h. (**K**) cytofluorimetric analysis of tumor-infiltrating myeloid cells; (**L**) percentage of tumor-infiltrating macrophages. Data are presented as median values ± SEM; n ≥ 3 mice per group. One-way ANOVA tests with Fisher's LSD test post hoc test were performed to obtain P values. (**p < 0.005; ***p < 0.001).

Supplementary Fig. S5

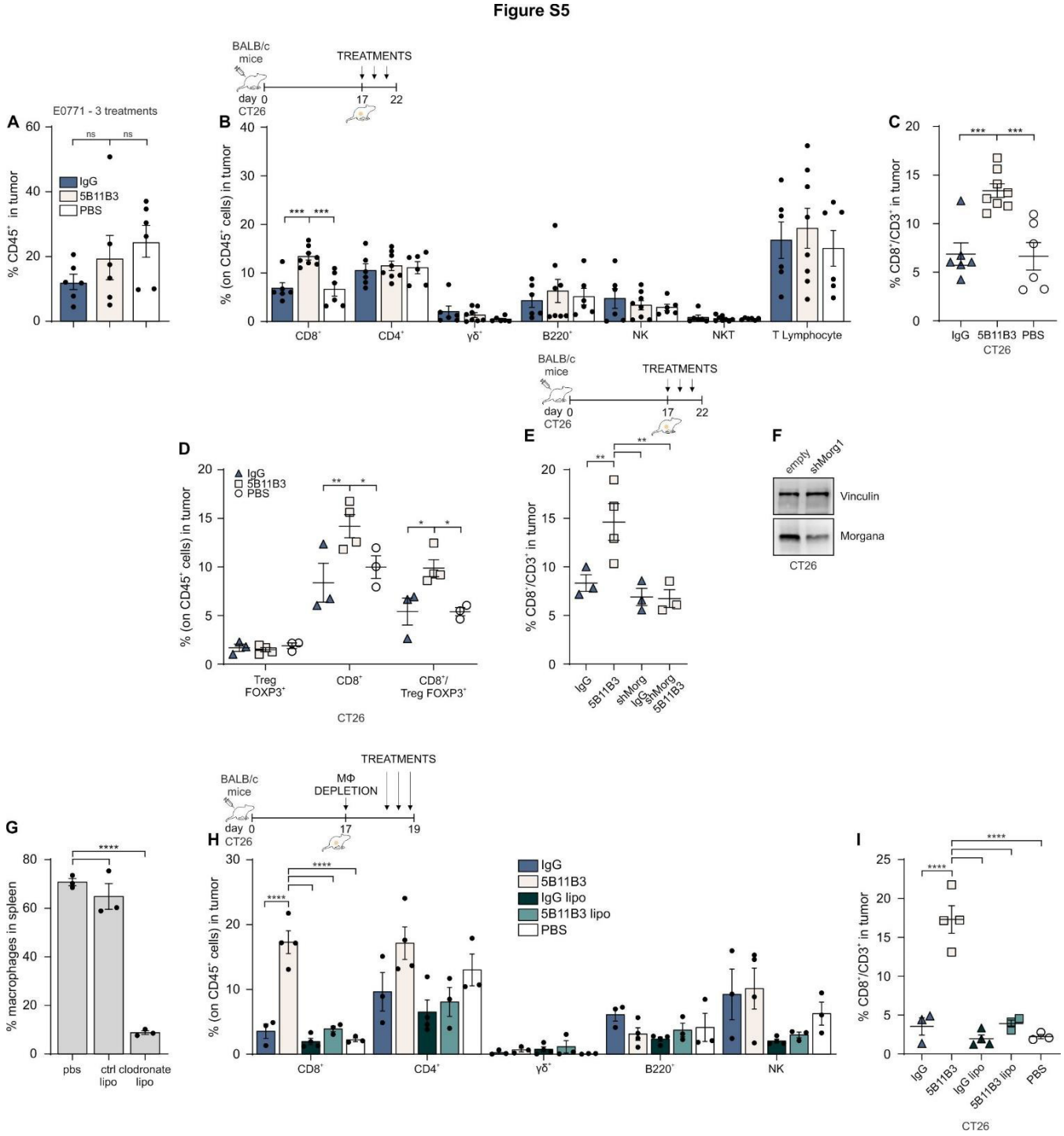

Supplementary Fig. S5. mAb 5B11B3 requires macrophages to induce CD8⁺ T lymphocytes recruitment in the primary tumor. (**A**) Percentage of CD45⁺ in the primary tumor of E0771 cancer

bearing mice, treated 3 times with mAb 5B11B3, IgG or PBS (100 μg, IV injection). Data are presented as median values ± SEM; n = 6 mice per group. (**B, C, D**) Identification of immune composition in the primary tumor after treatments with mAbs. (**B**) Percentage of immune cells, (**C**) of $CD8^+$ T lymphocytes and (**D**) of Treg $FOXP3^+$, $CD8^+$ T lymphocytes and the ratio of $CD8^+$ T lymphocytes/Treg $FOXP3^+$ in tumors of BALB/c mice subcutaneously inoculated with 2 x 10^5 CT26. After primary tumor development (size around 15 mm^3), animals were treated with mAb 5B11B3, IgG or PBS 3 times (100 μg, IV injection) and sacrificed. Data are presented as median values ± SEM; n ≥ 3 mice per group. One-way ANOVA tests with Fisher's LSD test post hoc test were performed to obtain P values. (**E-F**) Percentage of $CD8^+$ T lymphocytes in tumors of BALB/c mice subcutaneously inoculated with 2 x 10^5 CT26 empty or shMorg. (**E**) After primary tumor development (size around 15 mm^3), animals were treated with mAb 5B11B3 or control IgG 3 times (100 μg, IV injection) and sacrificed. Data are presented as median values ± SEM; n ≥ 3 mice per group. One-way ANOVA tests with Fisher's LSD test post hoc test were performed to obtain P values. (**F**) Western blot on CT26 infected with an empty lentiviral vector (empty) or a vector containing a shRNA for Morgana (shMorg1). Vinculin was used as loading control (**G**) Analysis of macrophage depletion in spleen of mice treated with clodronate liposomes, control liposomes (100 μg per 10 gr/mouse) or PBS. Data are presented as median values ± SEM; n = 3 mice per group. (**H**) Percentage of immune cells and (**I**) percentage of $CD8^+$ T lymphocytes in tumors of BALB/c mice subcutaneously inoculated with 2 x 10^5 CT26. After primary tumor development (size around 15 mm^3), animals were treated with clodronate liposomes in PBS (100 μg per 10 gr/mouse) and after 4 days mice were treated with mAb 5B11B3 or IgG (100 μg, IV injection) 3 times and sacrificed. Data are presented as median values ± SEM; n ≥ 3 mice per group. One-way ANOVA tests with Fisher's LSD test post hoc test were performed to obtain P values. (*$p < 0.05$; **$p < 0.005$; ***$p < 0.001$; ****$p < 0.0001$).

Supplementary Fig. S6

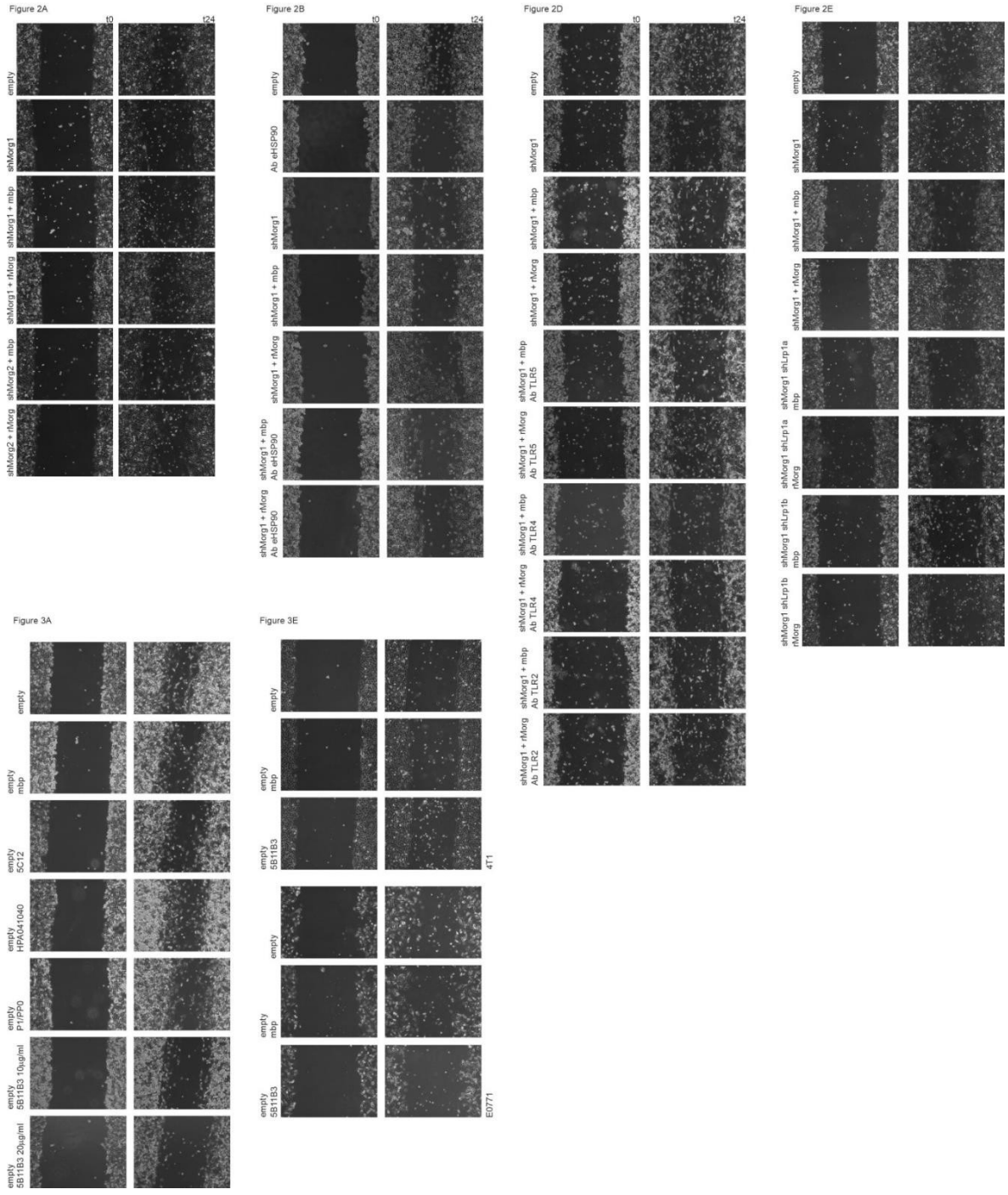

Supplementary Fig. S6. Wound healing representative images.

Supplementary Fig. S7

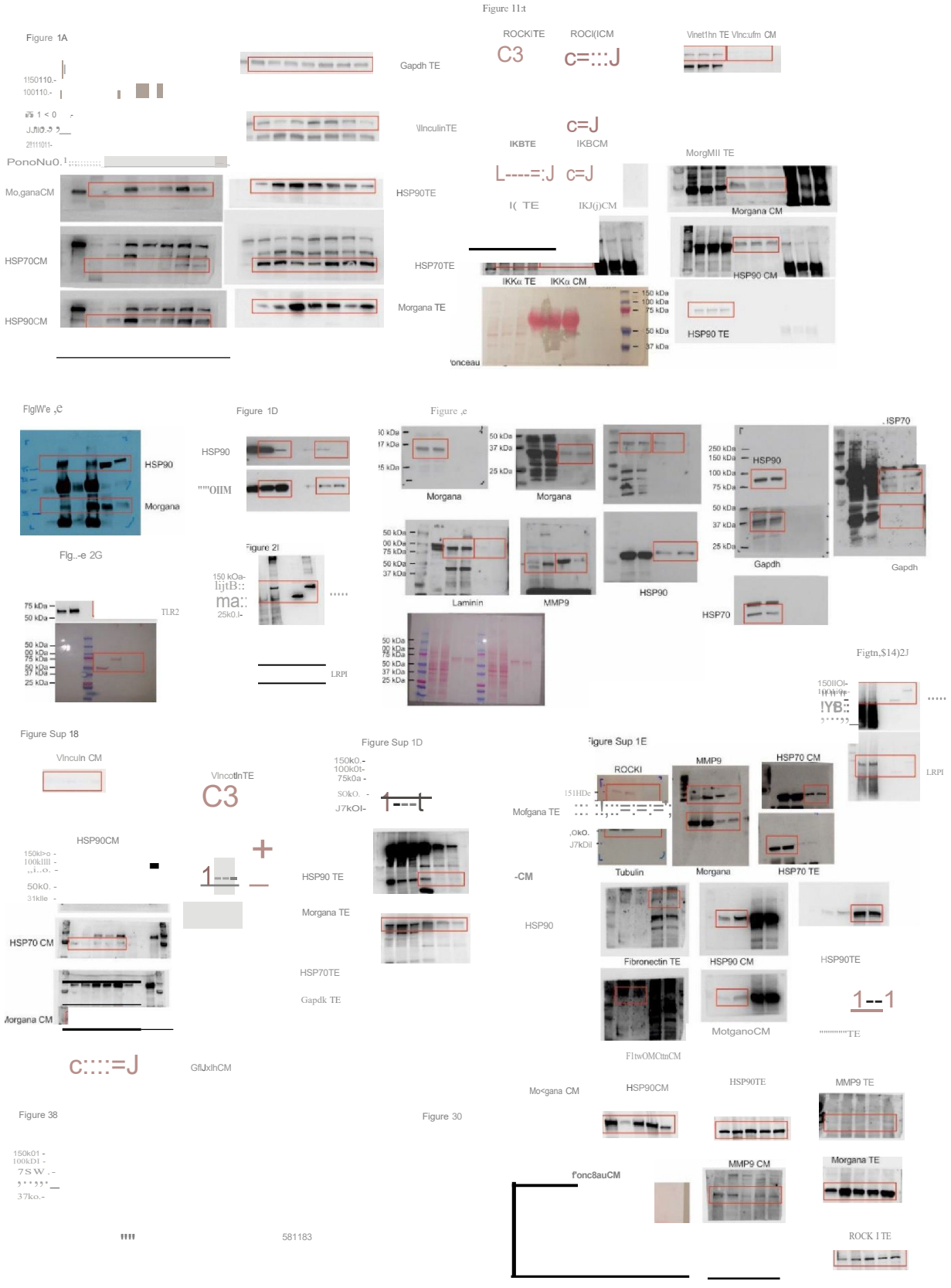

Supplementary Fig. S7. Uncropped images of Western blot analysis. Note that in some cases, nitrocellulose membranes had been probed with different antibodies in succession and residual bands of previous staining are visible.